Observational constraints on viable $f(R)$ parametrizations with geometrical and dynamical probes

Spyros Basilakos[*]

Academy of Athens, Research Center for Astronomy and Applied Mathematics, Soranou Efesiou 4, 11527 Athens, Greece

Savvas Nesseris[†]

Instituto de Física Teórica UAM-CSIC, Universidad Autonóma de Madrid, Cantoblanco, 28049 Madrid, Spain

Leandros Perivolaropoulos[‡]

Department of Physics, University of Ioannina, 45110 Ioannina, Greece
(Received 28 February 2013; published 24 June 2013)

We demonstrate that a wide range of viable $f(R)$ parametrizations (including the Hu and Sawicki and the Starobinsky models) can be expressed as perturbations deviating from the ΛCDM Lagrangian. We constrain the deviation parameter b using a combination of geometrical and dynamical observational probes. In particular, we perform a joint likelihood analysis of the recent type Ia supernova data, the cosmic microwave background shift parameters, the baryonic acoustic oscillations and the growth rate data provided by the various galaxy surveys. This analysis provides constraints for the following parameters: the matter density Ω_{m0}, the deviation from ΛCDM parameter b and the growth index $\gamma(z)$. We parametrize the growth index $\gamma(z)$ in three manners (constant, Taylor expansion around $z = 0$, and Taylor expansion around the scale factor). We point out the numerical difficulty for solving the generalized $f(R)$ Friedmann equation at high redshifts due to the stiffness of the resulting ordinary differential equation. We resolve this problem by constructing an efficient analytical perturbative method in the deviation parameter b. We demonstrate that this method is highly accurate, by comparing the resulting analytical expressions for the Hubble parameter with the numerical solutions at low and intermediate redshifts. Surprisingly, despite its perturbative nature, the accuracy of the method persists even for values of b that are of $O(1)$.

I. INTRODUCTION

A variety of cosmological studies have converged to a cosmic expansion history involving a spatially flat geometry and a cosmic dark sector formed by cold dark matter and some sort of dark energy, endowed with large negative pressure, in order to explain the observed accelerating expansion of the Universe [1–9]. In this framework, the absence of a fundamental physical theory, regarding the mechanism inducing the cosmic acceleration, has given rise to a plethora of alternative cosmological scenarios. Modified gravity models act as an important alternative to the scalar-field dark energy models, since they provide an efficient way of explaining the accelerated expansion of the Universe, under a modification of the nature of gravity. Such an approach is an attempt to evade the coincidence and cosmological constant problems of the standard ΛCDM model.

Particular attention over the last decades has been paid to $f(R)$ gravity theories [10]. In this scenario of nonstandard gravity, one modifies the Einstein-Hilbert action with a general function $f(R)$ of the Ricci scalar R. The $f(R)$ approach is a relatively simple but fundamental tool used to explain the accelerated expansion of the Universe. A pioneering approach was proposed long ago, where $f(R) = R + mR^2$ [11]. Later on, the $f(R)$ models were further explored from different points of view in Refs. [12–14] and a large number of functional forms of $f(R)$ gravity are currently available in the literature. It is interesting to mention that subsequent investigations [14] confirmed that $1/R$ gravity is an unacceptable model because it fails to reproduce the correct cosmic expansion in the matter era. Of course, there are many other possibilities to explain the present accelerating stage. Indeed, in the literature one can find a variety of modified gravity models (for reviews see Ref. [15]) which include the braneworld Dvali, Gabadadze and Porrati (hereafter DGP; Ref. [16]) model, Finsler-Randers gravity [17], scalar-tensor theories [18] and Gauss-Bonnet gravity [19].

The construction of observationally viable $f(R)$ theories has proved to be challenging because it has been shown [14] that most of these models do not predict a matter era in the cosmic expansion history. Nevertheless observationally viable $f(R)$ models have been constructed and two such examples are the following:

(1) The Hu and Sawicki (HS) model [20] with

[*]svasil@academyofathens.gr
[†]nesseris@nbi.ku.dk
[‡]leandros@uoi.gr

$$f(R) = R - m^2 \frac{c_1 (R/m^2)^n}{1 + c_2 (R/m^2)^n}, \qquad (1.1)$$

where c_1, c_2 are free parameters, $m^2 \simeq \Omega_{m0}H_0^2$ is of the order of the Ricci scalar R_0 at the present time, H_0 is the Hubble constant, Ω_{m0} is the dimensionless matter density parameter at the present time, and m and n are positive constants.

(2) The Starobinsky model [21] with

$$f(R) = R - c_1 m^2 [1 - (1 + R^2/m^4)^{-n}]. \quad (1.2)$$

These models were originally advertised as models that do not contain the cosmological constant as part of $f(R)$ being distinct from the ΛCDM form $f(R) = R - 2\Lambda$ (where Λ is the cosmological constant). However, it is straightforward to show that both the Hu and Sawicki and the Starobinsky models may be written in terms of ΛCDM modified by a distortion function $y(R, b)$ that depends on a deviation parameter b as

$$f(R) = R - 2\Lambda y(R, b), \quad (1.3)$$

where [22]

$$y(R, b) = 1 - \frac{1}{1 + (R/(b\Lambda))^n} \quad (1.4)$$

for the Hu and Sawicki model with $\Lambda = \frac{m^2 c_1}{2c_2}$ and $b = \frac{2c_2^{1-1/n}}{c_1}$, while

$$y(R, b) = 1 - \frac{1}{(1 + (\frac{R}{b\Lambda})^2)^n} \quad (1.5)$$

for the Starobinsky model where $\Lambda = \frac{c_1 m^2}{2}$ and $b = \frac{2}{c_1}$. Notice that in both cases the following two limits exist for $n > 0$:

$$\lim_{b\to 0} f(R) = R - 2\Lambda, \qquad \lim_{b\to\infty} f(R) = R, \quad (1.6)$$

and therefore both models reduce to ΛCDM for $b \to 0$. Notice that both the Hu and Sawicki and the Starobinsky models effectively include the cosmological constant even though they were advertised as being free from a cosmological constant in the original papers [20,21]. In fact by proper choices of the function $y(R, b)$ it is possible to construct infinite viable $f(R)$ models which however will always include ΛCDM as a limiting case for $b \to 0$.

Thus, an important question that arises is the following: What is the range of the deviation parameter b that is consistent with cosmological observations? This is the main question addressed in the present study. Since ΛCDM is consistent with observations we anticipate that the value $b = 0$ is within the acceptable range of b values. Thus, the interesting part of the question is, what is the maximum allowed value of b at eg the 2σ confidence level?

In order to address this question we solve the background modified Friedman equation assuming flatness and obtain the Hubble parameter $H(\Omega_{m0}, b; z)$. This involves the numerical solution of a stiff ordinary differential equation (ODE), second order in H, with initial conditions at high z that correspond to ΛCDM. The numerical solution of this stiff ODE at redshifts higher than $z \simeq 300$ is quite challenging. However, we have developed an efficient analytical perturbative expansion in b to solve it. This expansion leads to an analytic expression for $H(\Omega_{m0}, b; z)$ to all orders in b. We thus use geometric probes [type Ia surenovae (SnIa), the cosmic microwave background (CMB) shift parameter and baryon acoustic oscillation (BAO) data] to constrain the parameters Ω_{m0}, b that appear in the expression of $H(\Omega_{m0}, b; z)$.

In addition to geometric observations that probe the cosmic metric directly, dynamical probes play a crucial role in constraining cosmological models. The growth index, γ, could provide an efficient way to discriminate between modified gravity models and scalar field dark energy (hereafter DE) models which adhere to general relativity. The accurate determination of the growth index is considered one of the most fundamental tasks for observational cosmology. Its importance stems from the fact that there is only a weak dependence of γ on the equation of state (EoS) parameter $w(z)$, as has been found by Linder and Cahn [23], which implies that one can separate the background expansion history, $H(z)$, constrained by geometric probes (SnIa, BAO, CMB), from the fluctuation growth history, given by γ. For a constant DE equation of state w, it was theoretically shown that for DE models within general relativity the growth index γ is well approximated by $\gamma \simeq \frac{3(w-1)}{6w-5}$ (see Refs. [23–26]), which boils down to $\approx 6/11$ for the ΛCDM cosmology $w(z) = -1$. Notice, that in the case of the braneworld model of Dvali, Gabadadze and Porrati [16] we have $\gamma \approx 11/16$ (see also Refs. [23,27–29]), while for some $f(R)$ gravity models we have $\gamma \simeq 0.415 - 0.21z$ for various parameter values (see Refs. [30,31]). Recently, Basilakos and Stavrinos [32] found $\gamma \approx 9/14$ for the Finsler-Randers cosmology.

Observationally, indirect methods to measure γ have also been developed (mostly using a constant γ), based either on the observed growth rate of clustering [26,27,33–39] providing a wide range of γ values $\gamma \simeq (0.58–0.67)$, or on massive galaxy clusters (Vikhlinin *et al.* [40] and Rapetti *et al.* [41]). The latter study provides $\gamma = 0.42^{+0.20}_{-0.16}$. An alternative method for measuring γ involves weak gravitational lensing [42]. Gaztanaga *et al.* [43] performed a cross-correlation analysis between probes of weak gravitational lensing and redshift space distortions and found no evidence for deviations from general relativity. Also, Basilakos and Pouri [36] and Hudson and Turnbull [37] imposed constraints on the growth index using the combination parameter $F(z)\sigma_8(z)$,[1] of the growth rate of

---

[1] Here the capital $F(a)$ denotes the growth rate of structure. We follow the latter notation in order to avoid confusion with the $f(R)$.

structure $F(z)$ multiplied by the redshift-dependent rms fluctuations of the linear density field, $\sigma_8(z)$. The above authors found $\gamma = 0.602 \pm 0.05$ [36] and $\gamma = 0.619 \pm 0.05$ [37] while Basilakos and Pouri [36] showed that the current growth data can not accommodate the Dvali, Gabadadze and Porrati [16] gravity model.

In order to impose constraints on the viable $f(R)$ models discussed above, we use—in addition to geometric probes—the recent growth rate data as collected by Nesseris and Garcia-Bellido [44], Hudson and Turnbull [37] and Beutler *et al.* [45].

The plan of the paper is as follows. Initially in Sec. II, we briefly discuss the background cosmological equations. The basic features of the growth index are presented in Sec. III, where we extend the original Polarski and Gannouji method [46] for a general family of $\gamma(z)$ parametrizations as well as $f(R)$ cosmological models. In Sec. IV, a joint statistical analysis based on the *Union 2.1* set of type Ia supernovae [47], the observed baryonic acoustic oscillations [48], the shift parameter of the cosmic microwave background [9], and the observed linear growth rate of clustering, measured mainly from the PSCz, 2dF, VVDS, SDSS, 6dF, 2MASS, BOSS and WiggleZ redshift catalogs, is used to constrain the growth index model free parameters. Finally, we summarize our main conclusions in Sec. V.

II. THE BACKGROUND EVOLUTION

First of all we start with the assumption that the Universe is a self-gravitating fluid described by a modified gravity, namely $f(R)$ [10], and endowed with a spatially flat homogeneous and isotropic geometry. In addition, we also consider that the Universe is filled by nonrelativistic matter and radiation. The modified Einstein-Hilbert action reads

$$S = \int d^4 x \sqrt{-g} \left[\frac{1}{2k^2} f(R) + \mathcal{L}_m + \mathcal{L}_r \right], \quad (2.1)$$

where $\mathcal{L}_m$ is the Lagrangian of matter, $\mathcal{L}_r$ is the Lagrangian of radiation and $k^2 = 8\pi G$. Now by varying the action with respect to the metric[2] we arrive at

$$f_R G^\mu_\nu - g^{\mu\alpha} f_{R,\alpha;\nu} + \left[\frac{2\Box f_R - (f - R f_R)}{2} \right] \delta^\mu_\nu = k^2 T^\mu_\nu, \quad (2.2)$$

where R is the Ricci scalar, $f_R = \partial f / \partial R$, G^μ_ν is the Einstein tensor and T^μ_ν is the energy-momentum tensor of matter. Modeling the expanding Universe as a perfect fluid that includes radiation and cold dark matter with four-velocity U_μ, we have $T^\mu_\nu = -P g^\mu_\nu + (\rho + P) U^\mu U_\nu$, where $\rho = \rho_m + \rho_r$ and $P = p_m + p_r$ are the total energy density and pressure of the cosmic fluid respectively. Note that ρ_m is the matter density, ρ_r denotes the density of the

radiation and $p_m = 0$, $p_r = \rho_r/3$ are the corresponding pressures. Assuming negligible interaction between non-relativistic matter and radiation the Bianchi identity $\nabla^\mu T_{\mu\nu} = 0$ (which ensures the covariance of the theory) leads to the matter/radiation conservation laws,

$$\dot{\rho}_m + 3H\rho_m = 0, \qquad \dot{\rho}_r + 4H\rho_r = 0, \quad (2.3)$$

the solutions of which are $\rho_m = \rho_{m0} a^{-3}$ and $\rho_r = \rho_{r0} a^{-4}$. Note that the over-dot denotes a derivative with respect to the cosmic time t, $a(t)$ is the scale factor and $H \equiv \dot{a}/a$ is the Hubble parameter.

Now, in the context of a flat Friedmann-Lemaître-Robertson-Walker metric with Cartesian coordinates

$$ds^2 = -dt^2 + a^2(t)(dx^2 + dy^2 + dz^2) \quad (2.4)$$

the Einstein tensor components are given by

$$G^0_0 = -3H^2, \qquad G^i_j = -\delta^i_j(2\dot{H} + 3H^2). \quad (2.5)$$

Inserting Eq. (2.5) into the modified Einstein field equation (2.2), for comoving observers, we derive the modified Friedmann equations

$$3f_R H^2 - \frac{f_R R - f}{2} + 3H f_{RR} \dot{R} = k^2(\rho_m + \rho_r), \quad (2.6)$$

$$-2f_R \dot{H} = k^2[\rho_m + (4/3)\rho_r] + \ddot{f}_R - H\dot{f}_R, \quad (2.7)$$

where $\dot{R} = aHdR/da$ and $f_{RR} = \partial^2 f / \partial R^2$. Also, the contraction of the Ricci tensor provides the Ricci scalar,

$$R = g^{\mu\nu} R_{\mu\nu} = 6 \left(\frac{\ddot{a}}{a} + \frac{\dot{a}^2}{a^2} \right) = 6(2H^2 + \dot{H}). \quad (2.8)$$

Of course, if we consider $f(R) = R$ then the field equation (2.2) boil down to the nominal Einstein equations, a solution of which is the Einstein-de Sitter model. On the other hand, the concordance Λ cosmology is fully recovered for $f(R) = R - 2\Lambda$. We would like to stress here that within the context of the metric formalism the above $f(R)$ cosmological models must simultaneously obey some strong conditions (for an overall discussion see Ref. [15]). Briefly these are the following. (i) $f_R > 0$ for $R \geq R_0 > 0$, where R_0 is the Ricci scalar at the present time. If the final attractor is a de Sitter point we need to have $f_R > 0$ for $R \geq R_1 > 0$, where R_1 is the Ricci scalar at the de Sitter point. (ii) $f_{RR} > 0$ for $R \geq R_0 > 0$. (iii) $f(R) \approx R - 2\Lambda$ for $R \gg R_0$. (iv) $0 < \frac{R f_{RR}}{f_R}(r) < 1$ at $r = -\frac{R f_R}{f} = -2$.

Finally, from the current analysis it becomes clear that unlike the standard Friedmann equations in Einstein's general relativity the modified equations of motion (2.6) and (2.7) are complicated and thus it is difficult to solve them analytically. Below, we are going to compare the $f(R)$ results with those of the concordance ΛCDM model. This can help us to understand better the theoretical basis of the current $f(R)$ models as well as the variants from general relativity.

---

[2]We use the metric i.e. the Hilbert variational approach.

For practical reasons (see below), we derive the effective ("geometrical") dark energy EoS parameter in terms of $E(a) = H(a)/H_0$ (see Refs. [15,49] and references therein),

$$w(a) = \frac{-1 - \frac{2}{3}a\frac{d\ln E}{da}}{1 - \Omega_m(a)}, \qquad (2.9)$$

where

$$\Omega_m(a) = \frac{\Omega_{m0}a^{-3}}{E^2(a)}. \qquad (2.10)$$

Differentiating the latter and utilizing Eq. (2.9) we find that

$$\frac{d\Omega_m}{da} = \frac{3}{a}w(a)\Omega_m(a)[1 - \Omega_m(a)]. \qquad (2.11)$$

In the case of the traditional ΛCDM cosmology $f(R) = R - 2\Lambda$, the corresponding dark energy EoS parameter is strictly equal to -1 and the normalized Hubble function in the matter era is given by

$$E_\Lambda(a) = (\Omega_{m0}a^{-3} + 1 - \Omega_{m0})^{1/2}. \qquad (2.12)$$

A. The $f(R)$ functional forms

In order to solve numerically the modified Friedmann equation (2.6) we need to know a priori the functional form of $f(R)$. Due to the absence of a physically well-motivated functional form for the $f(R)$ parameter, there are many theoretical propositions in the literature. In this paper for the background we use different reference expansion models, namely flat ΛCDM and $f(R)$ respectively. Below we briefly present the two most popular $f(R)$ models whose free parameters can be constrained from the current cosmological data.

Firstly, we use the Hu and Sawicki [20] model (hereafter f_1CDM) as expressed by equation (1.1). Using the constraints provided by the violations of the weak and strong equivalence principle, Capozziello and Tsujikawa [50] found that $n > 0.9$. On the other hand it has been proposed in Ref. [51] that n is an integer number, so for simplicity in our work we have set $n = 1$. In Ref. [20] the parameters (c_1, c_2) were related to Ω_{m0}, Ω_{r0} and the first derivative of $f(R)$ at the present epoch f_{R0} in order to ensure the expansion history is close to that of ΛCDM. Specifically, we have

$$\frac{c_1}{c_2} = 6\frac{(1 - \Omega_{r0} - \Omega_{m0})}{\Omega_{m0}},$$

$$f_{R0} = 1 - \frac{nc_1}{c_2^2}\left(-9 + \frac{12}{\Omega_{m0}} - \frac{12\Omega_{r0}}{\Omega_{m0}}\right)^{-1-n}.$$

The first two derivatives of Eq. (1.1) with respect to R are

$$f_R = \frac{R[c_2(\frac{R}{m^2})^n + 1]^2 - c_1 m^2 n(\frac{R}{m^2})^n}{R[c_2(\frac{R}{m^2})^n + 1]^2}, \qquad (2.13)$$

$$f_{RR} = \frac{c_1 m^2 n(\frac{R}{m^2})^n[c_2(n+1)(\frac{R}{m^2})^n - n + 1]}{R^2[c_2(\frac{R}{m^2})^n + 1]^3}. \qquad (2.14)$$

As discussed in the Introduction, the Lagrangian of Eq. (1.1) can also be written as

$$\begin{aligned} f(R) &= R - \frac{m^2 c_1}{c_2} + \frac{m^2 c_1/c_2}{1 + c_2(R/m^2)^n} \\ &= R - 2\Lambda\left(1 - \frac{1}{1 + (R/(b\Lambda))^n}\right) \\ &= R - \frac{2\Lambda}{1 + (\frac{b\Lambda}{R})^n}, \end{aligned} \qquad (2.15)$$

where $\Lambda = \frac{m^2 c_1}{2c_2}$ and $b = \frac{2c_2^{1-1/n}}{c_1}$. In this form it is clear that the HS model can be arbitrarily close to ΛCDM, depending on the parameters b and n.

We now consider the Starobinsky [21] model (hereafter f_2CDM) as expressed by equation (1.2): as in the Hu and Sawicki [20] model we choose $m^2 \simeq \Omega_{m0}H_0^2$, while Ref. [50] also showed that $n > 0.9$. In this case the f_R and f_{RR} derivatives are given by

$$f_R = 1 - \frac{2nR(1 + \frac{R^2}{m^4})^{-1-n}c_1}{m^2}, \qquad (2.16)$$

$$f_{RR} = -\frac{2m^2 n(1 + \frac{R^2}{m^4})^{-n}[m^4 - (1 + 2n)R^2]c_1}{(m^4 + R^2)^2}. \qquad (2.17)$$

In order to ensure that the expansion history of this model is close to that of ΛCDM we need to match the c_1 constant to Λ, i.e. $-c_1 m^2 = -2\Lambda = -6(1 - \Omega_{m0} - \Omega_{r0})H_0^2$ or

$$c_1 = \frac{6(1 - \Omega_{m0} - \Omega_{r0})}{\Omega_{m0}}. \qquad (2.18)$$

As discussed in the Introduction, the Lagrangian of Eq. (1.2) can also be written as

$$f(R) = R - 2\Lambda\left[1 - \frac{1}{(1 + (\frac{R}{b\Lambda})^2)^n}\right], \qquad (2.19)$$

where $\Lambda = \frac{c_1 m^2}{2}$ and $b = \frac{2}{c_1}$. In this form it is clear that this model can also be arbitrarily close to ΛCDM, depending on the parameters b and n. Thus, the parameter b determines how close the model is to ΛCDM.

It is interesting to mention that the above $f(R)$ models satisfy all the strong conditions (see Sec. II) and thus they provide predictions which are similar to those of the usual (scalar field) DE models, as far as the cosmic history (presence of the matter era, stability of cosmological perturbations, stability of the late de Sitter point, etc.) is concerned. Also, we will restrict our present numerical solutions to the choice $H_0 = 70.4$ Km/s/Mpc and $\sigma_8 = 0.8$.[3] For example, in this case the modified

---

[3]We treat σ_8 as a free parameter at the end of Sec. IV B 2.

Friedmann equations for the $f(R)$ models contain two free parameters, namely (Ω_{m0}, b) which can be constrained from the current cosmological data.

B. Analytic approximations

In this subsection we present a novel approximation scheme for the solution of the modified Friedmann equation (2.6) and we explicitly apply it to the two widely used models (2.16) and (2.19).

In particular we may write Eq. (2.6) as

$$-f_R H^2(N) + (\Omega_{m0}e^{-3N} + \Omega_{r0}e^{-4N}) + \frac{1}{6}(f_R R - f)$$
$$= f_{RR} H^2(N) R'(N), \qquad (2.20)$$

where the prime denotes differentiation with respect to N and $R(N)$ is given by Eq. (2.8). Using now Eq. (1.3) for specific $f(R)$ models, the above ODE [and its solution $H(N)$] may be expanded around ΛCDM with respect to the deviation parameter b.

Since we are interested in testing deviations from the ΛCDM model, we find it useful to perform a series expansion of the solution of the ODE (2.20) around $b = 0$ as

$$H^2(N) = H_\Lambda^2(N) + \sum_{i=1}^{M} b^i \delta H_i^2(N), \qquad (2.21)$$

where

$$\frac{H_\Lambda^2(N)}{H_0^2} = \Omega_{m0}e^{-3N} + \Omega_{r0}e^{-4N} + (1 - \Omega_{m0} - \Omega_{r0})$$
$$(2.22)$$

and M is the number of terms we keep before truncating the series. Usually keeping only the two first nonzero terms is more than enough to have excellent agreement of *better than* 0.001% at all redshifts with the numerical solution for realistic values of the parameter $b \in [0.001, 0.5]$.

By expanding Eq. (2.20) with Eq. (2.21) to any given order in b we can find analytical solutions for the Hubble expansion rate. It is easy to show that for the HS model and for $n = 1$ the first two terms of the expansion are the following:

$$H_{HS}^2(N) = H_\Lambda^2(N) + b\,\delta H_1^2(N) + b^2\delta H_2^2(N) + \cdots, \qquad (2.23)$$

where $\delta H_1^2(N)$ and $\delta H_2^2(N)$ are given by Eqs. (A1) and (A2) respectively. For the Starobinsky model for $n = 1$ we have

$$H_{\text{Star}}^2(N) = H_\Lambda^2(N) + b^2\delta H_2^2(N) + b^4\delta H_4^2(N) + \cdots, \qquad (2.24)$$

where $\delta H_2^2(N)$ and $\delta H_4^2(N)$ are given by Eqs. (A3) and (A4) respectively.

Obviously, similar expressions can be obtained for any $f(R)$ model and up to any order provided that for $b \to 0$ we obtain ΛCDM. We stress that the expressions for $\delta H_i^2(N)$ are algebraic up to all orders, something that makes this method very useful and fast compared to solving the differential equation numerically. Furthermore, this method avoids another problem of the numerical integration, namely that at very high redshifts the ODE of Eq. (2.6) is quite stiff, thus making the integration impossible with standard methods. This makes the numeric solution quite time consuming and possibly unreliable, something which as we will show is not a problem for our analytic approximation.

In what follows we will test the validity of this approximation in both cases. In order to do this we compared the predictions of the analytical solutions of Eqs. (2.23) and (2.24) to the numerical solution in each case for a large variety of values for the parameter b. In particular, we estimated the average percent deviation between the approximations and the numerical solution, defined as

$$\langle \text{error}(b) \rangle = \left\langle 100 \cdot \left(1 - \frac{H_{\text{approx}}(z, b)}{H_{\text{numeric}}(z, b)}\right) \right\rangle, \qquad (2.25)$$

where the average is taken over redshifts in the range $z \in [0, 30]$. The reason for averaging is that most of the data we will use involve distance scales, like the luminosity distance, that are integrals of the Hubble parameter. We have also kept z below 200 since the numerical ODE solver of MATHEMATICA is unable to go to larger redshifts due to the stiffness of the ODE.

We show the results of the average error for a large variety of values of the parameter $b \in [0.01, 2]$ in Fig. 1. Clearly, the approximation behaves exceptionally well within the ranges of interest, i.e. the vertical dashed lines. These regions correspond, as we will see in a later section, to the best-fit values of b. The horizontal dotted line indicates an error of 10^{-5}%. Finally, we see that our approximation is on average in agreement to better than ~ 0.01% for realistic parameters, i.e. $b \sim O(1)$, of the $f(R)$ models. In a forthcoming paper we attempt to investigate the validity of our method against all the available $f(R)$ gravity models.

We should note that there is some similarity between the iterative approach suggested by Starobinsky in Ref. [52] and our method. Both approaches are based on taking small deviations from an unperturbed simple case. However, our approach is based on the existence of a well-defined dimensionless deviation parameter b while Starobinsky uses the WKB approximation with no reference to a deviation perturbative parameter. In addition, in Ref. [52] the iterative procedure was based on the assumption that the Ricci scalar can be written in terms of three components, namely $R^{(0)}$, δR_{ind} and δR_{osc} [see Starobinsky's Eq. 12], whereas in our approach we perform a Taylor expansion of the Hubble function around $b = 0$. The reason for using such an
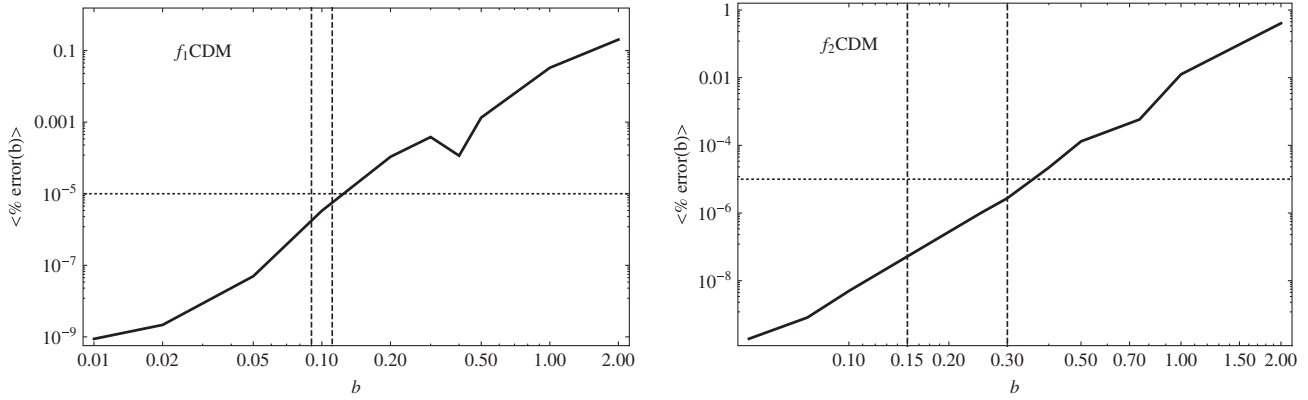
FIG. 1.   The results of the average error in the redshift range $z \in [0, 30]$ for a large variety of values of the parameter $b \in [0.01, 2]$. Clearly, the approximation behaves exceptionally well within the ranges of interest, i.e. the vertical dashed lines. The horizontal dotted line indicates an error of $10^{-5}\%$.

expansion is due to the fact that for b close to zero both $f(R)$ models tend to the concordance ΛCDM model.

Our approach is indeed a perturbative approach and it should be applicable for small values of the deviation parameter b. The fact that the method remains accurate even for values of b of $O(1)$ can be attributed to the fact that even for b of $O(1)$ the deviation term as a whole remains small. As expected, however, the accuracy of the method decreases for increasing b (see Fig. 1). We will compare the above iterative procedures in a forthcoming paper.

III. THE EVOLUTION OF THE LINEAR GROWTH FACTOR

In this section we concentrate on the subhorizon scales in which the DE component is expected to be homogeneous and thus we can use perturbations only on the matter component of the cosmic fluid [53]. Therefore, the evolution equation of the matter fluctuations, for cosmological models where the DE fluid has a vanishing anisotropic stress and the matter fluid is not coupled to other species (see Refs. [30,54–59]), is given by

$$\ddot{\delta}_m + 2H\dot{\delta}_m = 4\pi G_{\mathrm{eff}}\rho_m\delta_m \qquad (3.1)$$

where ρ_m is the matter density and $G_{\mathrm{eff}}(t) = G_N Q(t)$, with G_N denoting Newton's gravitational constant.

For those cosmological models which adhere to general relativity, $[Q(t) = 1, G_{\mathrm{eff}} = G_N]$, the above equation reduces to the usual time-evolution equation for the mass density contrast [60], while in the case of modified gravity models (see Refs. [23,30,54,58]), we have $G_{\mathrm{eff}} \neq G_N$ (or $Q \neq 1$). Indeed it has been shown (see Refs. [30,31]) that in the case of $f(R)$ models the quantity Q is a function of the scale factor and of the wave number κ,

$$Q(a, \kappa) = \frac{1}{f_R} \frac{1 + 4\frac{\kappa^2}{a^2}\frac{f_{RR}}{f_R}}{1 + 3\frac{\kappa^2}{a^2}\frac{f_{RR}}{f_R}}. \qquad (3.2)$$

We restrict our analysis to the choice of $\kappa = 1/\lambda = 0.1h\,\mathrm{Mpc}^{-1}$ or $\lambda = 10h^{-1}\,\mathrm{Mpc}$ (see also Ref. [61]).

In this context, $\delta_m(t) \propto D(t)$, where $D(t)$ is the linear growing mode (usually scaled to unity at the present time). Of course, solving Eq. (3.1) for the concordance Λ cosmology, we derive the well-known perturbation growth factor (see Ref. [60]),

$$D_\Lambda(z) = \frac{5\Omega_{m0}E_\Lambda(z)}{2} \int_z^{+\infty} \frac{(1 + u)du}{E_\Lambda^3(u)}. \qquad (3.3)$$

In this work we use the above equation normalized to unity at the present time.

Since in most of the cases Eq. (3.1) does not yield analytical solutions, it is common in this kind of study to provide an efficient parametrization of the matter perturbations that is based on the growth rate of clustering [60],

$$F(a) = \frac{d\ln\delta_m}{d\ln a} \simeq \Omega_m^\gamma(a), \qquad (3.4)$$

where γ is the growth index (see Refs. [23–26,54]) which plays a key role in cosmological studies as we described in the Introduction.

A. The generalized growth index parametrization

Inserting the first equality of Eq. (3.4) into Eq. (3.1) and using simultaneously Eq. (2.9) and $\frac{d}{dt} = H\frac{d}{d\ln a}$, we derive, after some algebra, that

$$a\frac{dF}{da} + F^2 + X(a)F = \frac{3}{2}\Omega_m(a)Q(a), \qquad (3.5)$$

with

$$X(a) = \frac{1}{2} - \frac{3}{2}w(a)[1 - \Omega_m(a)], \qquad (3.6)$$

where in order to evaluate the final form of Eq. (3.6) we have used Eq. (2.11).

Now, we consider that the growth index varies with cosmic time. Transforming Eq. (3.5) from a to redshift $[\frac{d}{da} = -(1+z)^{-2}\frac{d}{dz}]$ and utilizing Eqs. (3.4) and (2.11) we simply derive the evolution equation of the growth index $\gamma = \gamma(z)$ (see also Ref. [46]). Indeed this is given by

$$-(1+z)\gamma'\ln(\Omega_m) + \Omega_m^\gamma + 3w(1-\Omega_m)\left(\gamma - \frac{1}{2}\right) + \frac{1}{2}$$
$$= \frac{3}{2}Q\Omega_m^{1-\gamma}, \tag{3.7}$$

where a prime denotes a derivative with respect to redshift. At the present time the above equation becomes

$$-\gamma'(0)\ln(\Omega_{m0}) + \Omega_{m0}^{\gamma(0)} + 3w_0(1-\Omega_{m0})\left[\gamma(0) - \frac{1}{2}\right] + \frac{1}{2}$$
$$= \frac{3}{2}Q_0\Omega_{m0}^{1-\gamma(0)}, \tag{3.8}$$

where $Q_0 = Q(z=0, \kappa)$ and $w_0 = w(z=0)$.

In this work we phenomenologically parametrize $\gamma(z)$ by the following general relation (see Ref. [36]):

$$\gamma(z) = \gamma_0 + \gamma_1 y(z). \tag{3.9}$$

Obviously, the above equation can be viewed as a first-order Taylor expansion around some cosmological quantity such as $a(z)$, z and $\Omega_m(z)$. We would like to stress that for those $y(z)$ functions which satisfy $y(0) = 0$ [or $\gamma(0) = \gamma_0$] one can write the parameter γ_1 in terms of γ_0. In this case $[\gamma'(0) = \gamma_1 y'(0)]$, using Eq. (3.8) we obtain

$$\gamma_1 = \frac{\Omega_{m0}^{\gamma_0} + 3w_0(\gamma_0 - \frac{1}{2})(1 - \Omega_{m0}) - \frac{3}{2}Q_0\Omega_{m0}^{1-\gamma_0} + \frac{1}{2}}{y'(0)\ln\Omega_{m0}}. \tag{3.10}$$

Let us now briefly present various forms of $\gamma(z)$, $\forall\ z$.
(i) Constant growth index (hereafter Γ_0 model): Here we set γ_1 strictly equal to zero, thus $\gamma = \gamma_0$.
(ii) Expansion around $z = 0$ (see Ref. [46]; hereafter Γ_1 model): In this case we have $y(z) = z$. Note, however, that this parametrization is valid at relatively low redshifts $0 \leq z \leq 0.5$. In the statistical analysis presented below we utilize a constant growth index, namely $\gamma = \gamma_0 + 0.5\gamma_1$ for $z > 0.5$.
(iii) Expansion around $a = 1$ ([62–64]; hereafter Γ_2 model): Here the function y becomes $y(z) = 1 - a(z) = \frac{z}{1+z}$. Obviously, at large redshifts $z \gg 1$ we get $\gamma_\infty \simeq \gamma_0 + \gamma_1$.

For the Γ_1 and Γ_2 parametrizations one can easily show that $y(0) = 0$ and $y'(0) = 1$, respectively. As an example, for the case of the ΛCDM cosmology with $\gamma_0 \simeq 6/11$ and $\Omega_{m0} = 0.273$, Eq. (3.10) provides $\gamma_1 \simeq -0.0478$. In addition, based on Starobinsky's $f(R)$ model with $(\Omega_{m0}, \gamma_0) = (0.273, 0.415)$ Gannouji *et al.* [30] found $\gamma_1 = -0.21$.

Finally, we should note that the growth index is clearly model dependent via γ_1, as can be seen from Eqs. (3.9) and (3.10). However, Gannouji *et al.* [30] found that in the case of the Starobinsky $f(R)$ model the corresponding growth rate of clustering [see Eq. (3.4)] is not really affected by the scale especially up to $z = 2$ (see their Fig. 2). In addition, we have demonstrated that the allowed deviation from ΛCDM is relatively small in the cases considered (b less than 0.5 at 2σ in most cases) and therefore any allowed scale dependence of the growth is minor. This implies that the use of the value of the measured $f\sigma_8$ can be used without sacrifice of accuracy.

Another issue concerning nonlinear effects is that in this work we utilize $\kappa = 1/\lambda = 0.1h\,\text{Mpc}^{-1}$ which corresponds to $\lambda = 10h^{-1}\,\text{Mpc}$. Note that the power-spectrum normalization σ_8 which is the rms mass fluctuation on $R_8 = 8h^{-1}\,\text{Mpc}$ corresponds to $\kappa = 0.125h\,\text{Mpc}^{-1}$.
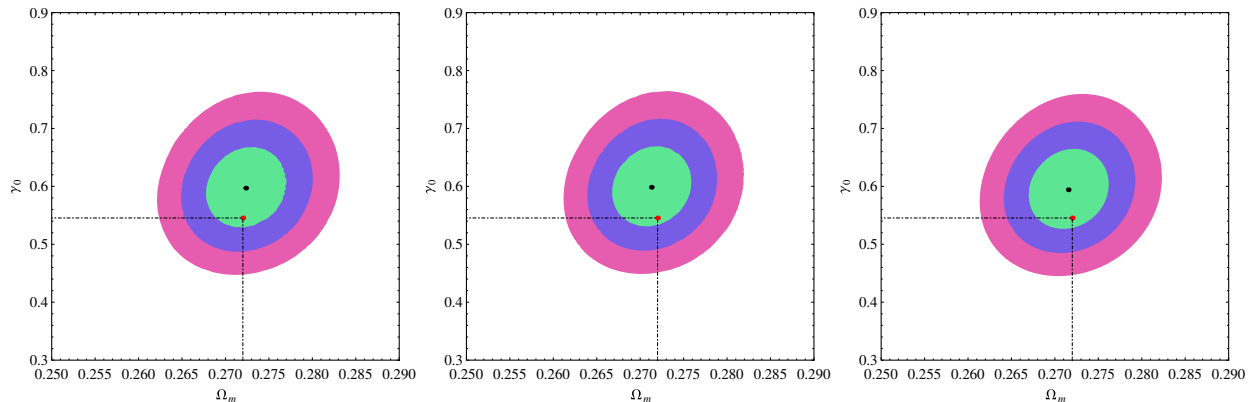

FIG. 2 (color online).   Left: Likelihood contours for χ^2 equal to 2.30, 6.18 and 11.83, corresponding to 1σ, 2σ and 3σ confidence levels, in the (Ω_{m0}, γ) plane using a ΛCDM expansion model. Middle and Right: Here we show the corresponding contours in the case of $f(R)$ models (f_1CDM in the middle panel and f_2CDM in the right panel). In all cases the red point corresponds to $(\Omega_{m0}, \gamma) = (0.272, 6/11)$. In this plot and in the ones that follow we have set the parameters that are not shown (e.g. b) to their best-fit values for the corresponding model (see Table III). Here we use $n = 1$.

On the other hand it has been common practice to assume that the shape of the power spectrum recovered from galaxy surveys matches the linear matter power spectrum shape on scales $\kappa \lesssim 0.15h\,\mathrm{Mpc}^{-1}$ ([65,66]; see also the discussion in Sec. IV of Ref. [67]). Obviously the choice of $\kappa = 0.1h\,\mathrm{Mpc}^{-1}$ ensures that we are treating the liner regime. Of course we have repeated our analysis for different values of κ and we confirm the results of Gannouji *et al.*, i.e. that small variations around $\kappa = 0.1h\,\mathrm{Mpc}^{-1}$ do not really affect the qualitative evolution of the growth rate of clustering and thus of γ. Furthermore, we find that the evolution of $G_{\mathrm{eff}}(z)$ is almost completely unaffected for different values of κ; see for example Fig. 9 (top) and Fig. 10.

Nevertheless, we do anticipate a minor contribution of nonlinear effects even on these scales at a level less than a few percent [68]. These effects would tend to slightly amplify the value of γ and increase the error bars correspondingly by less than a few percent.

IV. OBSERVATIONAL CONSTRAINTS

In the following we briefly present some details of the statistical method and on the observational sample that we adopt in order to constrain the free parameters of the growth index, presented in the previous section.

A. The growth data

The growth data that we utilize in this article based on the PSCz, 2dF, VVDS, SDSS, 6dF, 2MASS, BOSS and WiggleZ galaxy surveys, for which their combination parameter of the growth rate of structure, $F(z)$, and the redshift-dependent rms fluctuations of the linear density field, $\sigma_8(z)$, is available as a function of redshift, $F(z)\sigma_8(z)$. The $F\sigma_8 \equiv \mathrm{f}\sigma_8$ estimator is almost a model-independent way of expressing the observed growth history of the Universe (see Ref. [69]). Indeed the observed growth rate of structure ($F_{\mathrm{obs}} = \beta\mathcal{B}$) is derived from the redshift space-distortion parameter $\beta(z)$ and the linear bias $\mathcal{B}$. Observationally, using the anisotropy of the correlation function one can estimate the $\beta(z)$ parameter. On the other hand, the linear bias factor can be defined as the ratio of the variances of the tracer (galaxies, quasistellar objects, etc.) and underlying mass density fields, smoothed at $8h^{-1}\,\mathrm{Mpc}$, $\mathcal{B}(z) = \sigma_{8,\mathrm{tr}}(z)/\sigma_8(z)$, where $\sigma_{8,\mathrm{tr}}(z)$ is measured directly from the sample. Combining the above definitions we arrive at $\mathrm{f}\sigma_8 \equiv F\sigma_8 = \beta\sigma_{8,\mathrm{tr}}$. We would like to point out that the different cosmologies (including those of modified gravity) enter only weakly in the observational determination of $\beta(z)$ (and thus of $\mathrm{f}\sigma_8$), through the definition of distances. In Table I we quote the precise numerical values of the data points with the corresponding errors and references.

B. The overall likelihood analysis

In order to constrain the cosmological parameters and the growth index of the $f(R)$ models one needs to perform a joint likelihood analysis, involving the cosmic expansion data, such as SnIa, BAO and the CMB shift parameter together with the growth data. Up to now, due to the large errors of the growth data with respect to the cosmic expansion data, various authors preferred to first constrain Ω_{m0} using SnIa/BAO/CMB and then to use the growth data alone. Of course, armed with the recent high-quality growth data it would be worthwhile to simultaneously constrain (Ω_{m0}, b, γ). In particular, we use the *Union 2.1* set of 580 SnIa of Suzuki *et al.* [47],[4] and the observed BAOs. For simplicity, but without loss of generality, we only considered the case where the covariance matrix of the SnIa data is diagonal. The BAO data are given in terms of the parameter $d_z(z) = \frac{l_{\mathrm{BAO}}(z_{\mathrm{drag}})}{D_V(z)}$, where $l_{\mathrm{BAO}}(z_{\mathrm{drag}})$ is the BAO scale at the drag redshift, assumed known from CMB measurements, and [48]

$$D_V(z) = \left[(1+z)^2 D_A(z)^2 \frac{cz}{H(z)} \right]^{1/3} \qquad (4.1)$$

is the usual volume distance.

In this analysis we use the 6dF, the SDSS and WiggleZ BAO data shown in Table I. The WiggleZ collaboration [77] has measured the baryon acoustic scale at three different redshifts, complementing previous data at lower redshifts obtained by SDSS and 6DFGS [48].

The chi-square is given by

$$\chi^2_{\mathrm{BAO}} = \sum_{i,j} [d_i - d(z_i)] C_{ij}^{-1} [d_j - d(z_j)], \qquad (4.2)$$

where the indices i, j are in growing order in z, as in Table II. For the first six points, C_{ij}^{-1} was obtained from the covariance data in Ref. [77] in terms of d_z,

TABLE I. Summary of the observed growth rate and references.

Index	z	Growth Rate ($f\sigma_{8\mathrm{obs}}$)	References
1	0.02	0.360 ± 0.040	[37]
2	0.067	0.423 ± 0.055	[45]
3	0.17	0.510 ± 0.060	[69,70]
4	0.35	0.440 ± 0.050	[69,71]
5	0.77	0.490 ± 0.180	[33,69]
6	0.25	0.351 ± 0.058	[72]
7	0.37	0.460 ± 0.038	[72]
8	0.22	0.420 ± 0.070	[73]
9	0.41	0.450 ± 0.040	[73]
10	0.60	0.430 ± 0.040	[73]
11	0.78	0.380 ± 0.040	[73]
12	0.57	0.427 ± 0.066	[74]
13	0.30	0.407 ± 0.055	[75]
14	0.40	0.419 ± 0.041	[75]
15	0.50	0.427 ± 0.043	[75]
16	0.60	0.433 ± 0.067	[75]

---

[4]The SnIa data can be found at [76]and in Ref. [47].

$$C_{ij}^{-1} = \begin{pmatrix} 4444 & 0. & 0. & 0. & 0. & 0. \\ 0. & 30318 & -17312 & 0. & 0. & 0. \\ 0. & -17312 & 87046 & 0. & 0. & 0. \\ 0. & 0. & 0. & 23857 & -22747 & 10586 \\ 0. & 0. & 0. & -22747 & 128729 & -59907 \\ 0. & 0. & 0. & 10586 & -59907 & 125536 \end{pmatrix}. \tag{4.3}$$

The positions of CMB acoustic peaks are affected by the expansion history of the Universe from the decoupling epoch to today. In order to quantify the shift of acoustic peaks we use the data points $(l_a, \mathcal{R}, z_{\text{cmb}})$ of Ref. [78] (WMAP9), where l_a and $\mathcal{R}$ are two CMB shift parameters and z_{cmb} is the redshift at decoupling.

For the redshift z_{cmb} there is a fitting formula by Hu and Sugiyama [79],

$$z_{\text{cmb}} = 1048(1 + 0.00124\omega_b^{-0.738})(1 + g_1\omega_m^{g_2}), \tag{4.4}$$

where $g_1 = 0.0783\omega_b^{-0.238}/(1 + 39.5\omega_b^{0.763})$, $g_2 = 0.560/(1 + 21.1\omega_b^{1.81})$, $\omega_b \equiv \Omega_{b0}h^2$ and $\omega_m \equiv \Omega_{m0}h^2$ (h corresponds to the uncertainty of the Hubble parameter H_0 today, i.e. $H_0 = 100h \, \text{km} \, \text{sec}^{-1} \, \text{Mpc}^{-1}$).

For a flat prior, the 9-year WMAP data (WMAP9) measured best-fit values are [78]

$$\bar{V}_{\text{CMB}} = \begin{pmatrix} l_a \\ \mathcal{R} \\ z_{cmb} \end{pmatrix} = \begin{pmatrix} 302.40 \\ 1.7246 \\ 1090.88 \end{pmatrix}. \tag{4.5}$$

The corresponding inverse covariance matrix is [78]

$$C_{\text{CMB}}^{-1} = \begin{pmatrix} 3.182 & 18.253 & -1.429 \\ 18.253 & 11887.879 & -193.808 \\ -1.429 & -193.808 & 4.556 \end{pmatrix}. \tag{4.6}$$

We thus define

$$X_{\text{CMB}} = \begin{pmatrix} l_a - 302.40 \\ \mathcal{R} - 1.7246 \\ z_{cmb} - 1090.88 \end{pmatrix}, \tag{4.7}$$

and construct the contribution of CMB to χ^2 as

$$\chi_{\text{CMB}}^2 = X_{\text{CMB}}^T C_{\text{CMB}}^{-1} X_{\text{CMB}}. \tag{4.8}$$

TABLE II. The BAO data used in this analysis. The first six data points are volume averaged and correspond to Table 3 of Ref. [77]. Their inverse covariance matrix is given by Eq. (4.3).

	6dF	SDSS		WiggleZ		
z	0.106	0.2	0.35	0.44	0.6	0.73
d_z	0.336	0.1905	0.1097	0.0916	0.0726	0.0592
Δd_z	0.015	0.0061	0.0036	0.0071	0.0034	0.0032

Notice that χ_{CMB}^2 depends on the parameters $(\Omega_{m0}, \Omega_{b0}, h)$. The density parameter of radiation today is

$$\Omega_{r0} = \Omega_{\gamma0}(1 + 0.2271N_{\text{eff}}), \tag{4.9}$$

where $\Omega_{\gamma0}$ is the photon density parameter and N_{eff} is the relativistic degrees of freedom. We adopt the standard values $\Omega_{\gamma0} = 2.469 \times 10^{-5}h^{-2}$ and $N_{\text{eff}} = 3.04$ [78]. Concerning the constraints on the parameters assuming a fixed H_0 value we should note that the statistical analysis does not depend on an a priori selected value of H_0. First, the SnIa distance moduli are always normalized using the internally determined H_0. On the other hand one of the merits of using the shift parameter in cosmological studies is that its dependence on the Hubble constant is almost negligible (for details see Ref. [80]). Indeed one can see from Eq. (4.4) that we use the normalized cosmological parameters $\omega_m = \Omega_{m0}h^2$ and $\omega_b = \Omega_{b0}h^2$. In this context, the H_0 dependence does enter in the analysis of the CMB shift parameter via Ω_{r0} [see Eq. (4.9)], but small variations around $\sim 70 \, \text{km/sec/Mpc}$ are not expected to affect the qualitative results.

The overall likelihood function[5] is given by the product of the individual likelihoods according to

$$\mathcal{L}_{\text{tot}}(\mathbf{p_1}, \mathbf{p_2}) = \mathcal{L}_E(\mathbf{p_1}) \times \mathcal{L}_f(\mathbf{p_1}, \mathbf{p_2}), \tag{4.10}$$

where $\mathcal{L}_f$ refers to the dynamical probe likelihood fit and

$$\mathcal{L}_E(\mathbf{p_1}) = \mathcal{L}_{\text{SNIa}} \times \mathcal{L}_{\text{BAO}} \times \mathcal{L}_{\text{CMB}}. \tag{4.11}$$

The vectors $\mathbf{p_1}$, $\mathbf{p_2}$ contain the free parameters of the $f(R)$ model and depend on the model. In particular, the essential free parameters that enter in the theoretical expectation are $\mathbf{p_1} \equiv (\Omega_{m0}, b)$ and $\mathbf{p_2} \equiv (\gamma_0, \gamma_1)$. Note that in the case of the ΛCDM we have $\mathbf{p_1} \equiv \Omega_{m0}$. Also, in all cases we have set $\sigma_8 = 0.8$.

Since likelihoods are defined as $\mathcal{L} \propto \exp(-\chi^2/2)$; this translates into an addition for the joint χ_{tot}^2 function,

$$\chi_{\text{tot}}^2(\mathbf{p_1}, \mathbf{p_2}) = \chi_E^2(\mathbf{p_1}) + \chi_f^2(\mathbf{p_1}, \mathbf{p_2}), \tag{4.12}$$

with

$$\chi_E^2(\mathbf{p_1}) = \chi_{\text{SNIa}}^2 + \chi_{\text{BAO}}^2 + \chi_{\text{CMB}}^2. \tag{4.13}$$

---

[5]Likelihoods are normalized to their maximum values. In the present analysis we always report 1σ uncertainties on the fitted parameters.

The minimization of the χ^2_{tot} was done in MATHEMATICA. Note that the χ^2_f is given by

$$\chi^2_f(\mathbf{p_1}, \mathbf{p_2}, z_i) = \sum_{i=1}^{N_f}\left[\frac{f\sigma_{8_{\text{obs}}}(z_i) - f\sigma_8(\mathbf{p_1}, \mathbf{p_2}, z_i)}{\sigma_i}\right]^2,$$

(4.14)

where σ_i is the observed growth-rate uncertainty.

To this end, since $N/n_{\text{fit}} > 40$ we will use—relevant to our case—the *corrected* Akaike information criterion (AIC) [81], defined, for the case of Gaussian errors, as

$$\text{AIC} = \chi^2_{\text{min}} + 2n_{\text{fit}} \tag{4.15}$$

where $N = N_{\text{EXP}} + N_f$ and n_{fit} is the number of free parameters. A smaller value of the AIC indicates a better model-data fit. However, small differences in the AIC are not necessarily significant and therefore, in order to assess the effectiveness of the different models in reproducing the data, one has to investigate the model pair difference $\Delta \text{AIC} = \text{AIC}_y - \text{AIC}_x$. The higher the value of $|\Delta \text{AIC}|$, the higher the evidence against the model with a higher value of the AIC, with a difference $|\Delta \text{AIC}| \gtrsim 2$ indicating a positive evidence and $|\Delta \text{AIC}| \gtrsim 6$ indicating a strong evidence, while a value $\lesssim 2$ indicates consistency among the two comparison models. A numerical summary of the statistical analysis for the background expansion models as well as for the various $\gamma(z)$ parametrizations is shown in Table III.

At this point we should stress that in this work we only use the shift parameter and do not use the full CMB likelihood provided by CAMB. The reason for this is that our analysis has demonstrated self-consistently that only small deviations from ΛCDM are allowed. Thus the use of the shift parameter for this range of small deviations is expected to be an acceptable approximation to the more accurate (but also more complicated) full CMB likelihood approach.

Furthermore, we have decided to utilize (as many authors did in the past) the CMB shift parameter which is a valid and frequently used tool in this kind of study, especially over the last decade. The robustness of the shift parameter was tested and discussed in Ref. [82] and it has been found that the shift parameter changes when massive neutrinos are included (which is not our case here) or when there is a strongly varying equation of state parameter [the $f(R)$ models remain close to ΛCDM].

1. Constant growth index

First of all we utilize the Γ_0 parametrization ($\gamma = \gamma_0$, $\gamma_1 = 0$: see Sec. III A). Therefore, the corresponding f_1CDM and f_2CDM statistical vectors $\mathbf{p_2}$ contain only three free parameters, namely $\mathbf{p_2} \equiv (\mathbf{p_1}, \gamma_0, 0)$, where $\mathbf{p_1} \equiv (\Omega_{m0}, b)$. Accordingly, if we consider the ΛCDM model then $\mathbf{p_1} \equiv \Omega_{m0}$, implying that the vector $\mathbf{p_2}$ includes two free parameters.

Our main results are listed in Table II, where we quote the best-fit parameters with the corresponding 1σ uncertainties, for three different expansion models. In Fig. 2 we present the 1σ, 2σ and 3σ confidence levels in the (Ω_{m0}, γ) plane. It becomes evident that by using the most recent growth data set together with the expansion cosmological data we can place strong constraints on (Ω_{m0}, γ). In all cases the best-fit value $\Omega_{m0} = 0.272 \pm 0.003$ is in very good agreement with that provided by WMAP9 + SPT + ACT ($\Omega_{m0} = 0.272$; Hinshaw *et al.* [78]).

Concerning the ΛCDM expansion model (see the right panel of Fig. 2) our growth index results are in agreement within 1σ errors to those of Samushia *et al.* [72] who found $\gamma = 0.584 \pm 0.112$, and to those of Ref. [38] who obtained $\Omega_{m0} = 0.273 \pm 0.011$ and $\gamma = 0.586 \pm 0.080$. However, our best-fit value $\gamma = 0.597 \pm 0.046$ is somewhat greater than the theoretically predicted value of $\gamma_\Lambda \simeq 6/11$ (see lines in the right panel of Fig. 2). Such a small discrepancy between the theoretical ΛCDM and the observationally fitted value of γ has also been found by other authors. For example, Di Porto and Amendola [34] obtained

TABLE III. Statistical results for the combined growth data (see Table I): The first column indicates the expansion model, the second column corresponds to $\gamma(z)$ parametrizations appearing in Sec. III A. The third and fourth columns provide the Ω_{m0} and b best values. The fifth and sixth columns show the γ_0 and γ_1 best-fit values. In all cases we used $\sigma_8 = 0.8$. The remaining columns present the goodness-of-fit statistics (χ^2_{min}, AIC and $|\Delta \text{AIC}| = |\text{AIC}_\Lambda - \text{AIC}_{f(R)}|$).

Exp. Model	Param. Model	Ω_{m0}	b	γ_0	γ_1	χ^2_{min}	AIC	$|\Delta\text{AIC}|$
ΛCDM	Γ_0	0.272 ± 0.003		0.597 ± 0.046	0	574.227	578.227	0
	Γ_1	0.272 ± 0.003		0.567 ± 0.066	0.116 ± 0.191	573.861	579.861	1.634
	Γ_2	0.272 ± 0.003		0.561 ± 0.068	0.183 ± 0.269	573.767	579.767	1.540
f_1CDM-[20]	Γ_0	0.271 ± 0.003	0.111 ± 0.140	0.598 ± 0.046	0	573.855	579.855	1.628
	Γ_1	0.271 ± 0.003	0.109 ± 0.142	0.573 ± 0.068	0.097 ± 0.195	573.633	581.633	3.406
	Γ_2	0.271 ± 0.003	0.109 ± 0.142	0.579 ± 0.070	0.101 ± 0.275	573.585	581.585	3.358
f_2CDM-[21]	Γ_0	0.272 ± 0.005	0.292 ± 0.647	0.594 ± 0.047	0	574.178	580.178	1.951
	Γ_1	0.272 ± 0.005	0.150 ± 1.355	0.567 ± 0.066	0.113 ± 0.199	573.857	581.857	3.630
	Γ_2	0.272 ± 0.005	0.149 ± 1.261	0.561 ± 0.068	0.179 ± 0.279	573.765	581.765	3.538
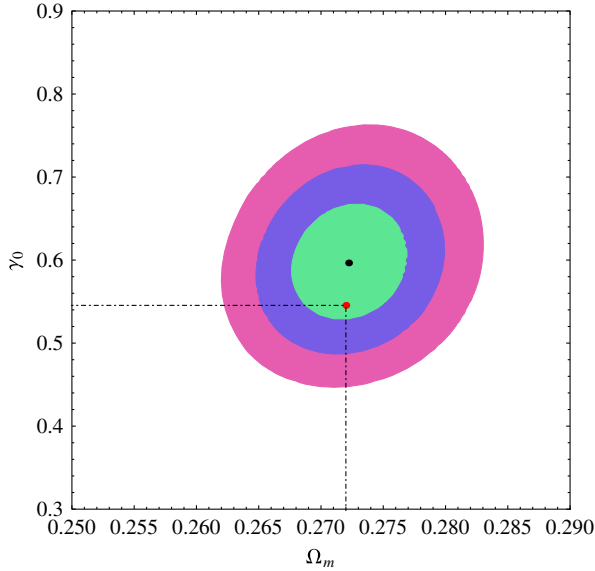
FIG. 3 (color online). The likelihood contours for χ^2 equal to 2.30, 6.18 and 11.83, corresponding to 1σ, 2σ and 3σ confidence levels, in the (Ω_{m0}, γ) plane in the case of the f_1CDM model for $n = 2$. In all cases the red point corresponds to $(\Omega_{m0}, \gamma) = (0.272, 6/11)$. Clearly, our results remain mostly unaffected by the choice of a particular n.

$\gamma = 0.60^{+0.40}_{-0.30}$, Gong [27] measured $\gamma = 0.64^{+0.17}_{-0.15}$ while Nesseris and Perivolaropoulos [26] found $\gamma = 0.67^{+0.20}_{-0.17}$. Recently, Basilakos and Pouri [36] and Hudson and Turnbull [37] using a similar analysis found $\gamma = 0.602 \pm 0.05$ and $\gamma = 0.619 \pm 0.054$ respectively. In this context, Samushia *et al.* [39] obtained $\gamma = 0.65 \pm 0.05$.

Concerning the f_1CDM model (see the middle panel of Fig. 2) the best-fit parameter is $\gamma_0 = 0.598 \pm 0.046$ with $\chi^2_{\min} \simeq 573.855$. Also, we checked the case where $n = 2$ (compare the middle plot of Fig. 2 with Fig. 3), and we found that our results remain mostly unaffected. Thus, throughout the rest of the paper we adopt $n = 1$. Also in the case of Starobinsky's f_2CDM model (see Fig. 2) the best-fit parameter is $\gamma_0 = 0.594 \pm 0.047$ with $\chi^2_{\min} \simeq 574.178$. In Fig. 4, we plot the measured $f\sigma_{8_{\mathrm{obs}}}(z)$ with the estimated growth-rate function, $f\sigma_8(z) = F(z)\sigma_8(z)$. The value of $\mathrm{AIC}_\Lambda (\simeq 578.227)$ is smaller than the corresponding $f(R)$ values which indicates that the ΛCDM model ($\gamma_\Lambda = 0.597$) appears now to fit the expansion and the growth data better than the f_1CDM and f_2CDM gravity models. The $|\Delta\mathrm{AIC}| = |\mathrm{AIC}_\Lambda - \mathrm{AIC}_{f_{1-2}(R)}|$ values (i.e., ~ 2) indicate that the growth data are consistent with the f_1CDM and f_2CDM gravity models with a constant growth index.

2. Time-varying growth index

Now we concentrate on the $\gamma(z)$ parametrizations, presented in Sec. III A. In this case the free parameters of the models are $\mathbf{p_2} \equiv (\Omega_{m0}, \gamma_0, \gamma_1)$ and $\mathbf{p_2} \equiv (\Omega_{m0}, b, \gamma_0, \gamma_1)$
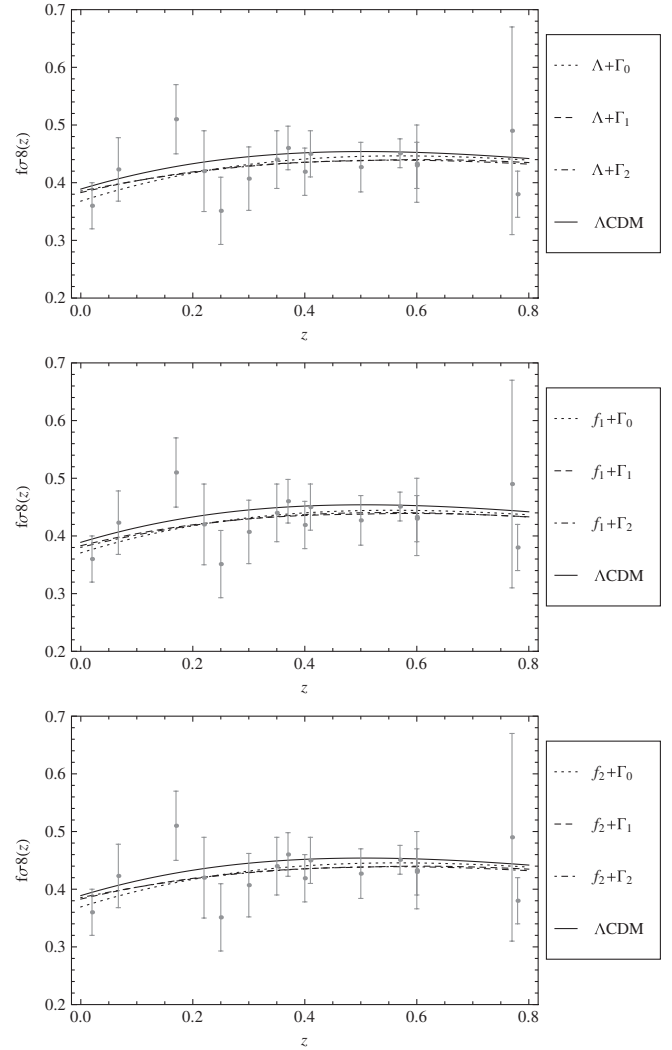

FIG. 4. Comparison of the observed and theoretical evolution of the growth rate $f\sigma_8(z) = F(z)\sigma_8(z)$. Top: The dotted, dashed and dot-dashed lines correspond to the best-fit Γ_0, Γ_1 and Γ_2 parametrizations with the background expansion given by ΛCDM, while the black line corresponds to the exact solution of Eq. (3.1) for $f\sigma_8(z)$ for the ΛCDM model for $\Omega_{m0} = 0.273$ [78]. Middle and Bottom: The dotted, dashed and dot-dashed lines correspond to the best-fit Γ_0, Γ_1 and Γ_2 parametrizations with the background expansion given by f_1CDM and f_2CDM respectively, while the black line corresponds to the exact solution of Eq. (3.1) for $f\sigma_8(z)$ for the ΛCDM model for $\Omega_{m0} = 0.272$ [78]. In all cases we utilize $\sigma_8 = 0.8$ and $n = 1$.

for the ΛCDM and f_1CDM, f_2CDM expansion models respectively.

In Fig. 5 (ΛCDM model), Fig. 6 (f_1CDM model) and Fig. 7 (f_2CDM model) we present the results of our statistical analysis for the Γ_1 (left panel) and Γ_2 (right panel) parametrizations in the (γ_0, γ_1) plane in which the corresponding contours are plotted for 1σ, 2σ and 3σ confidence levels. The theoretical (γ_0, γ_1) values (see Sec. IIi A) in the ΛCDM and $f(R)$ expansion models are
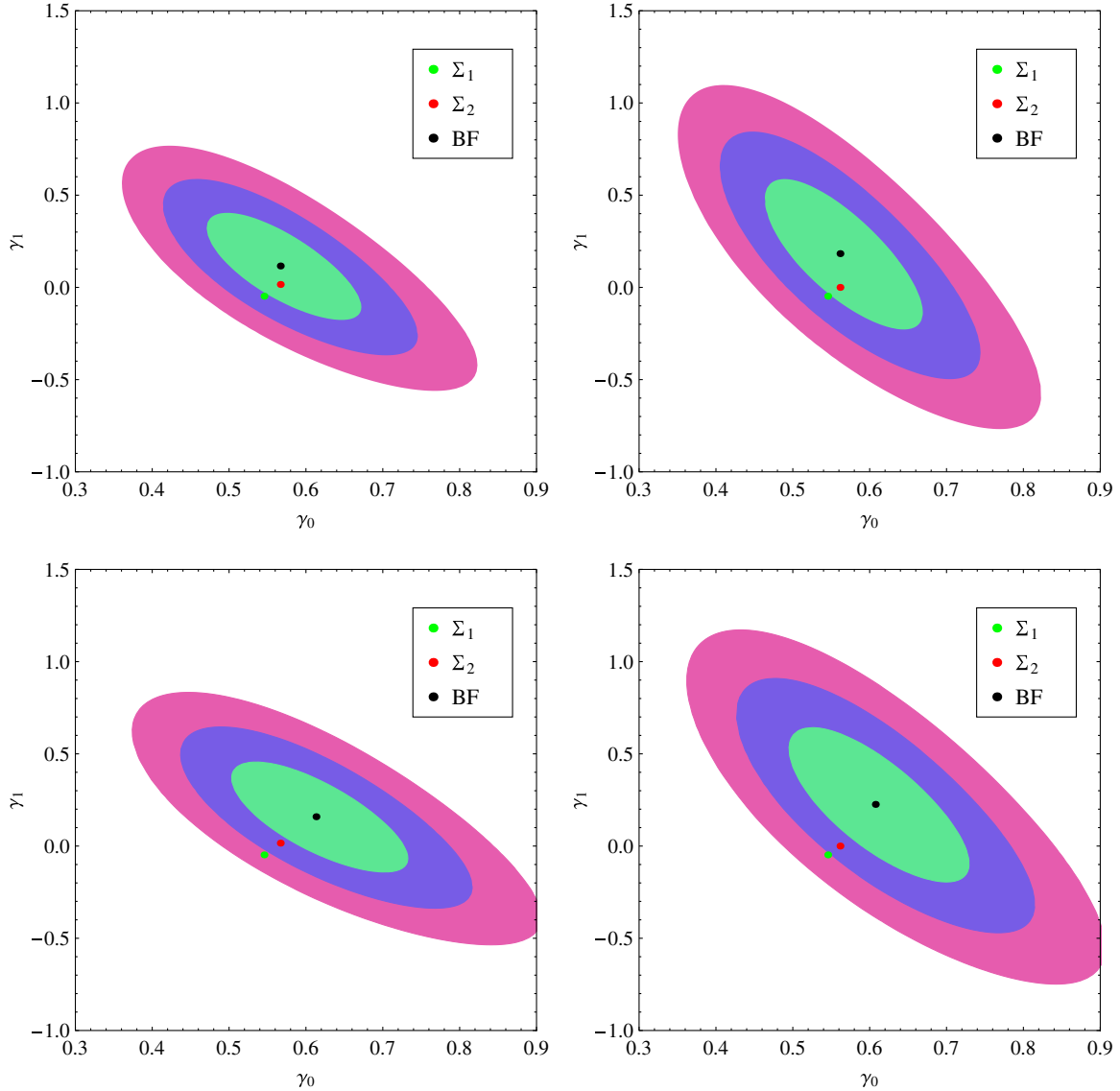
FIG. 5 (color online).   The ΛCDM *expansion model:* Likelihood contours (for $\Delta\chi^2 = -2\ln\mathcal{L}/\mathcal{L}_{\max}$ equal to 2.30, 6.18 and 11.83, corresponding to 1σ, 2σ and 3σ confidence levels) in the (γ_0, γ_1). The top row shows the contours when the rest of the parameters are fixed to their best-fit values, while the bottom row shows when they are marginalized over, while the left and right panels show the results based on the Γ_{1-2} parametrizations respectively. We also include the theoretical ΛCDM (γ_0, γ_1) values given in Sec. III, $\Sigma_1 = (6/11, \gamma_1(6/11, \Omega_{m0,bf}))$ and $\Sigma_2 = (\gamma_{0,bf}, \gamma_1(\gamma_{0,bf}, \Omega_{m0,bf}))$.

indicated by the colored dots. Overall, we find that the predicted ΛCDM, f_1CDM and f_2CDM (γ_0, γ_1) solutions of the Γ_{1-2} parametrizations are close to the 1σ borders ($\Delta\chi^2_{1\sigma} \simeq 2.30$; see green sectors in Figs. 5–7).

At this point we should mention that in all our contour plots, e.g. Fig. 2, we have fixed the various parameters to the best-fit values instead if marginalizing over them. It is well known in the literature (see for example Ref. [83]) that marginalizing over the nuisance parameters and fixing the parameter in general gives different effects since in the former case due to the integration of the likelihood points away from the best-fit and well within the tail of

the distribution they will contribute in the contour, thus creating a sort of a volume effect. Furthermore, we also show the corresponding $\gamma_0 - \gamma_1$ contours by marginalizing over the other parameters (see the bottom row in Fig. 5), and we find that both procedures are in good agreement within ~ 1–1.5σ. Statistically this means that the likelihood function is close to being a Gaussian.

Below we briefly discuss the main statistical results.

(a) Γ_1 parametrization: For the usual Λ cosmology the likelihood function peaks at $\gamma_0 = 0.567 \pm 0.066$ and $\gamma_1 = 0.116 \pm 0.191$ with $\chi^2_{\min} \simeq 573.861$. The latter results are in agreement with previous studies
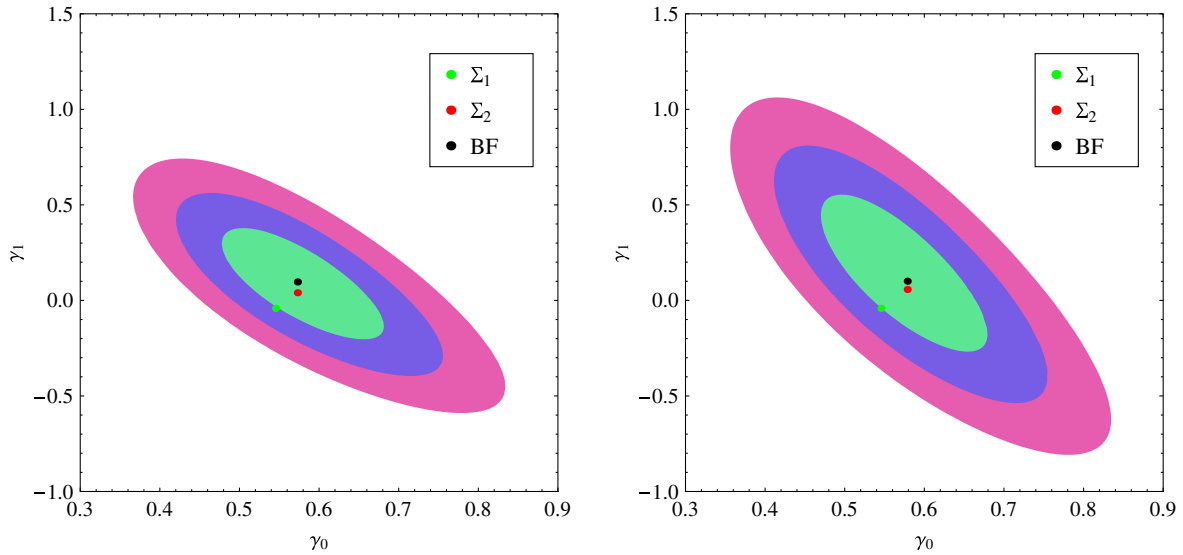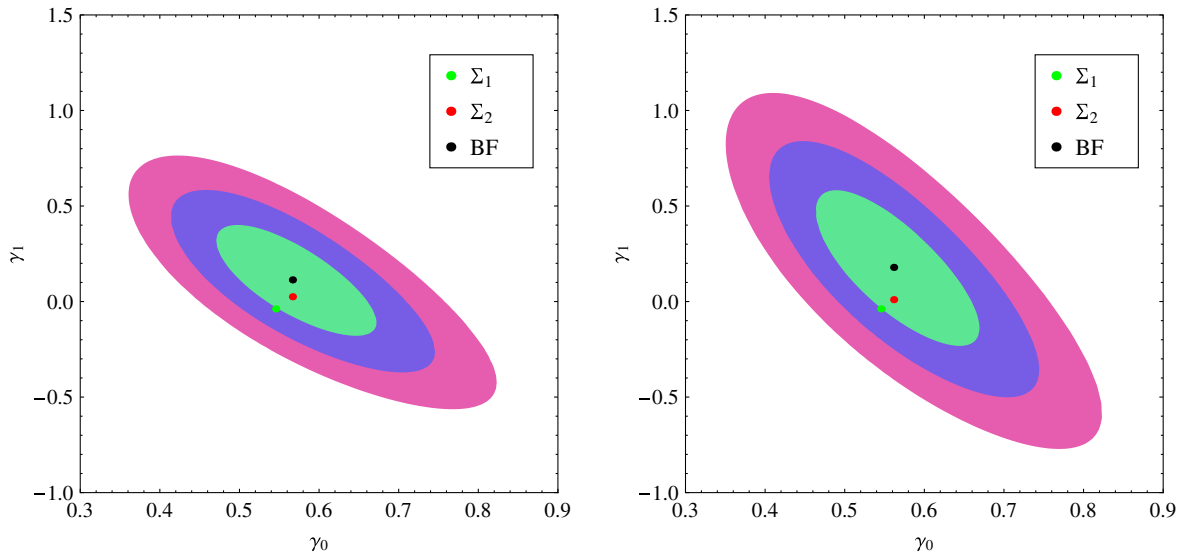
FIG. 6 (color online). The likelihood contours for the f_1CDM expansion model (for more definitions see caption of Fig. 5). Here the colored dots correspond to the theoretical f_1CDM (γ_0, γ_1) pair provided in Sec. III A, $\Sigma_1 = (6/11, \gamma_1(6/11, \Omega_{m0,bf}))$ and $\Sigma_2 = (\gamma_{0,bf}, \gamma_1(\gamma_{0,bf}, \Omega_{m0,bf}))$.

[26,34–36]. In the case of the f_1CDM and f_2CDM gravity models we find that $(\gamma_0, \gamma_1) = (0.573 \pm 0.068, 0.097 \pm 0.195)$ with $\chi^2_{min} \simeq 573.633$ and $(\gamma_0, \gamma_1) = (0.567 \pm 0.066, 0.113 \pm 0.199)$ and with $\chi^2_{min} \simeq 573.857$ respectively.

(b) Γ_2 parametrization: The best fit values are the following:

(i) For ΛCDM we have $\gamma_0 = 0.561 \pm 0.068$, $\gamma_1 = 0.183 \pm 0.269$ ($\chi^2_{min} \simeq 573.767$).

(ii) In the case of f_1CDM model we obtain $\gamma_0 = 0.579 \pm 0.070$, $\gamma_1 = 0.101 \pm 0.275$ ($\chi^2_{min} \simeq 573.585$).

(iii) For the f_2CDM gravity model we find $\gamma_0 = 0.561 \pm 0.068$, $\gamma_1 = 0.179 \pm 0.279$ ($\chi^2_{min} \simeq 573.765$).

Finally, as we have already mentioned in Table III, one may see a more compact presentation of our statistical results. In Fig. 8 we present the evolution of the growth index for various parametrizations. In all three cases of the concordance Λ and f_2CDM cosmological models (see upper and bottom panels of Fig. 8) the relative growth-index difference of the various fitted $\gamma(z)$ models indicates that the Γ_{1-2} parametrizations have a very similar redshift dependence for $z \leq 0.5$, while the Γ_2 parametrization

FIG. 7 (color online). The likelihood contours for the f_2CDM expansion model (for more definitions see caption of Fig. 5). Here the colored dots correspond to the theoretical f_2CDM (γ_0, γ_1) pair provided in Sec. III A, $\Sigma_1 = (6/11, \gamma_1(6/11, \Omega_{m0,bf}))$ and $\Sigma_2 = (\gamma_{0,bf}, \gamma_1(\gamma_{0,bf}, \Omega_{m0,bf}))$.
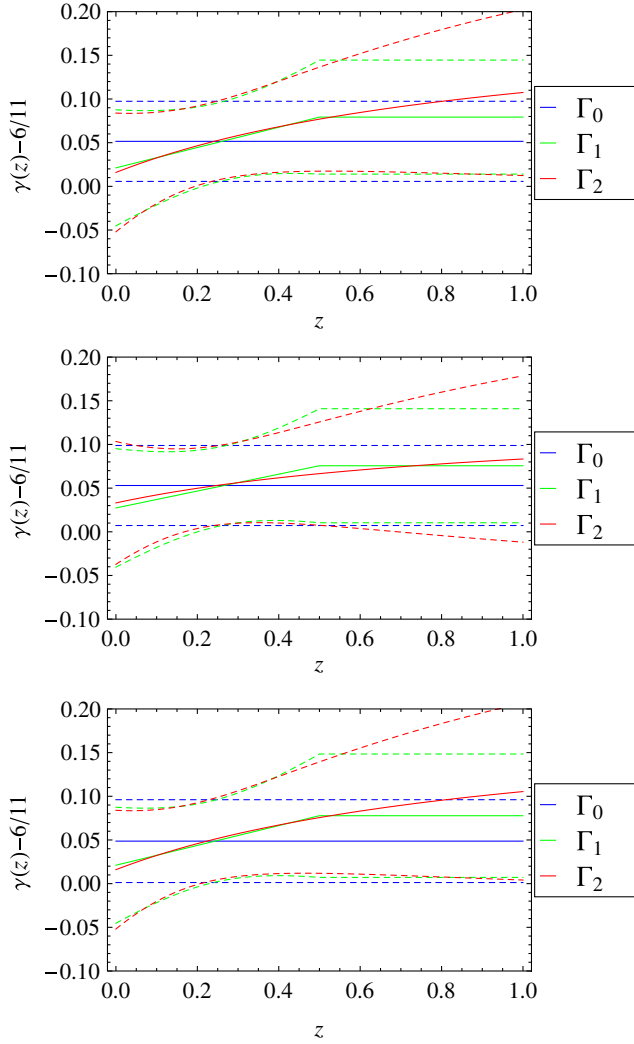
FIG. 8 (color online). Top: The evolution of the growth index $\gamma(z) - \frac{6}{11}$ for the ΛCDM model. The lines correspond to Γ_0 (blue), Γ_1 (green) and Γ_2 (red). Middle and Bottom: The evolution of the growth index for the f_1CDM and f_2CDM cosmological models, respectively. The lines correspond to Γ_0 (blue), Γ_1 (green) and Γ_2 (red). The dashed lines correspond to the 1σ errors.

shows very large deviations for $z > 0.5$. Based on the f_1CDM gravity model (middle panel of Fig. 8) we observe that the Γ_{1-2} parametrizations provide a similar evolution of the growth index.

Furthermore, in Fig. 9 we show the evolution of $G_{\mathrm{eff}}(z)$ for the two $f(R)$ models considered in the text: f_1CDM (left) and f_2CDM (right). The lines correspond to Γ_0 (blue), Γ_1 (green) and Γ_2 (red). As can be seen, both cases predict little evolution for $G_{\mathrm{eff}}(z)$ at late times, around 1.2% for f_1CDM and 0.5% for f_2CDM. Furthermore, while $G_{\mathrm{eff}}(z)$ shows almost the same evolution for all three parameterizations $\Gamma_{0,1,2}$ of f_1CDM, this is not the case for f_2CDM where Γ_0 differs significantly from the other two.

Finally, we repeated our analysis by treating σ_8 as a free parameter and the corresponding results are in good agreement with our previous analysis within 1σ with the results of Table III, thus justifying our choice to fix σ_8. Specifically, we found the following.

In the case of the ΛCDM:
(i) For the Γ_0 model, $\chi^2 = 573.254$, $\Omega_{m0} = 0.272 \pm 0.003$, $\gamma_0 = 0.523 \pm 0.0858$, $\sigma_8 = 0.761 \pm 0.038$.
(ii) For the Γ_1 model, $\chi^2 = 572.618$, $\Omega_{m0} = 0.272 \pm 0.003$, $\gamma_0 = 0.485 \pm 0.098$, $\gamma_1 = -0.398 \pm 0.502$, $\sigma_8 = 0.694 \pm 0.087$.
(iii) For the Γ_2 model, $\chi^2 = 572.652$, $\Omega_{m0} = 0.272 \pm 0.003$, $\gamma_0 = 0.483 \pm 0.097$, $\gamma_1 = -0.633 \pm 0.815$, $\sigma_8 = 0.685 \pm 0.097$.

In the case of the f_1CDM:
(i) For the Γ_0 model, $\chi^2 = 573.128$, $\Omega_{m0} = 0.271 \pm 0.003$, $b = 0.104 \pm 0.142$, $\gamma_0 = 0.533 \pm 0.089$, $\sigma_8 = 0.766 \pm 0.039$.
(ii) For the Γ_1 model, $\chi^2 = 573.277$, $\Omega_{m0} = 0.272 \pm 0.003$, $b = 0.086 \pm 0.143$, $\gamma_0 = 0.526 \pm 0.104$, $\gamma_1 = 0.054 \pm 0.507$, $\sigma_8 = 0.771 \pm 0.104$.
(iii) For the Γ_2 model, $\chi^2 = 572.452$, $\Omega_{m0} = 0.272 \pm 0.003$, $b = 0.072 \pm 0.144$, $\gamma_0 = 0.490 \pm 0.101$, $\gamma_1 = -0.679 \pm 0.835$, $\sigma_8 = 0.682 \pm 0.099$.

In the case of the f_2CDM:
(i) For the Γ_0 model, $\chi^2 = 573.766$, $\Omega_{m0} = 0.272 \pm 0.004$, $b = 0.109 \pm 1.48$, $\gamma_0 = 0.585 \pm 0.091$, $\sigma_8 = 0.786 \pm 0.041$.
(ii) For the Γ_1 model, $\chi^2 = 573.693$, $\Omega_{m0} = 0.272 \pm 0.002$, $b = 0.092 \pm 1.52$, $\gamma_0 = 0.549 \pm 0.108$, $\gamma_1 = 0.0934 \pm 0.551$, $\sigma_8 = 0.790 \pm 0.116$.
(iii) For the Γ_2 model, $\chi^2 = 572.653$, $\Omega_{m0} = 0.272 \pm 0.004$, $b = 0.082 \pm 1.71$, $\gamma_0 = 0.483 \pm 0.097$, $\gamma_1 = -0.635 \pm 0.408$, $\sigma_8 = 0.684 \pm 0.038$.

V. CONCLUSIONS

It is well known that the growth index γ plays a key role in cosmological studies because it can be used as a useful tool in order to test Einstein's general relativity on cosmological scales. In this article, we utilized the recent growth-rate data provided by clustering, measured mainly from the PSCz, 2dF, VVDS, SDSS, 6dF, 2MASS, BOSS and WiggleZ galaxy surveys, in order to constrain the growth index. In particular, we performed simultaneously a likelihood analysis of the recent expansion data (SnIa, CMB shift parameter and BAO) together with the growth rate of structure data, in order to determine the cosmological and the free parameters of the $\gamma(z)$ parametrizations and thus to statistically quantify the ability of $\gamma(z)$ to represent the observations. We considered the following growth index parametrization: $\gamma(z) = \gamma_0 + \gamma_1 y(z)$ [where $y(z) \equiv 0$, $y(z) = z$ and $1 - a(z)$]. Overall, considering a ΛCDM expansion model we found that the observed growth index is in agreement, within 1σ errors, with the theoretically predicted value of $\gamma_\Lambda \simeq 6/11$. Additionally, based on the Akaike information criterion we have shown that for any type of $\gamma(z)$ the combined analysis of the cosmological

(expansion+growth) data can accommodate the Hu-Sawicky and Starobinsky $f(R)$ gravity models for small values of the deviation parameter b.

Numerical analysis files: The MATHEMATICA and data files used for the numerical analysis of this study may be downloaded from [84].

ACKNOWLEDGMENTS

APPENDIX: USEFUL FORMULAS

Here we provide the exact expressions of the coefficients $\delta H_i^2(N)$ for the HS and Starobinsky models for $n = 1$. In all cases $H_\Lambda^2(N)$ is given by Eq. (2.22). For the HS model the first two terms are

$$\frac{\delta H_1^2(N)}{H_0^2} = -\frac{H_0^2(-1 + \Omega_{m0} + \Omega_{r0})^2(6H_\Lambda(N)^2 + 4H_\Lambda'(N)^2 + H_\Lambda(N)(15H_\Lambda'(N) + 2H_\Lambda''(N)))}{2H_\Lambda(N)(2H_\Lambda(N) + H_\Lambda'(N))^3}, \quad \text{(A1)}$$
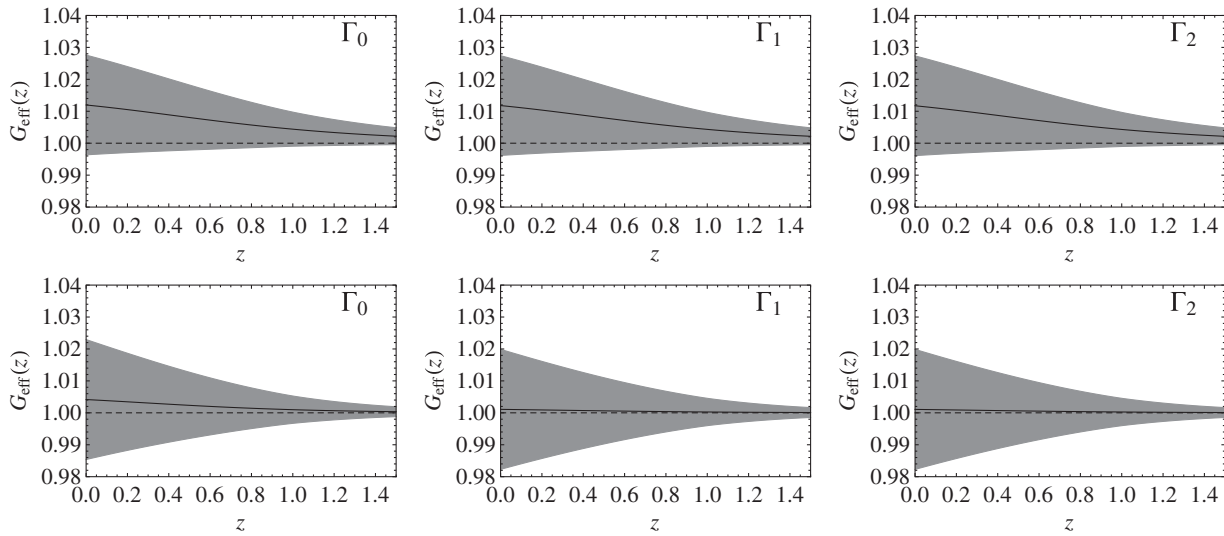

FIG. 9.   The evolution of the $G_{\text{eff}}(z)$ for the two $f(R)$ models considered in the text, f_1CDM (top) and f_2CDM (bottom), for all three growth rate parametrizations Γ_0 (left), Γ_1 (middle) and Γ_2 (right). In all cases we assume $\kappa = 0.1h$ Mpc^{-1}.
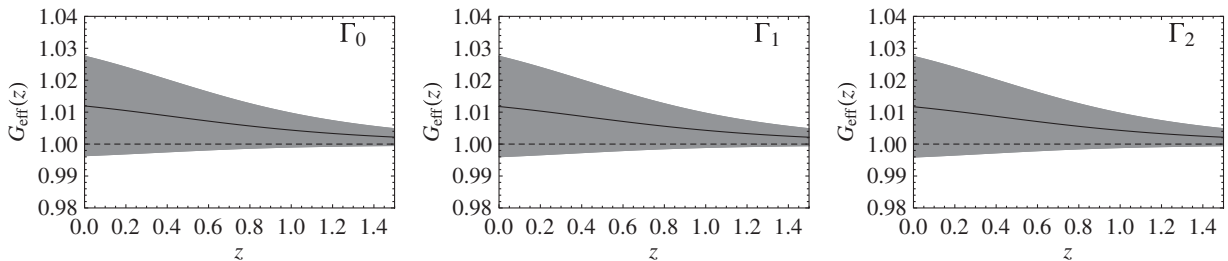

FIG. 10.   The evolution of the $G_{\text{eff}}(\kappa, z)$ for the HS $f(R)$ model for $\kappa = 0.01h$ Mpc^{-1}. The plot is practically indistinguishable from Fig. 9 (top). Therefore, we conclude that for these theories the particular choice of κ leaves the results unaffected.

$$
\begin{aligned}
\frac{\delta H_2^2(N)}{H_0^2} = &-(H_0^4(-1 + \Omega_m + \Omega_r)^3(128 H_\Lambda(N)^8 - 32 H_0^2(-1 + \Omega_m + \Omega_r)H_\Lambda'(N)^6 \\
&+ 32 H_\Lambda(N)^7(25 H_\Lambda'(N) + 3 H_\Lambda''(N)) - 2 H_0^2(-1 + \Omega_m + \Omega_r)H_\Lambda(N)H_\Lambda'(N)^4(139 H_\Lambda'(N) + 22 H_\Lambda''(N)) \\
&+ 16 H_\Lambda(N)^6(9 H_0^2(-1 + \Omega_m + \Omega_r) + 89 H_\Lambda'(N)^2 + 12 H_\Lambda'(N)H_\Lambda''(N)) \\
&+ H_\Lambda(N)^2 H_\Lambda'(N)^2(-749 H_0^2(-1 + \Omega_m + \Omega_r)H_\Lambda'(N)^2 + 9 H_\Lambda'(N)^4 - 48 H_0^2(-1 + \Omega_m + \Omega_r)H_\Lambda''(N)^2 \\
&- 4 H_0^2(-1 + \Omega_m + \Omega_r)H_\Lambda'(N)(74 H_\Lambda''(N) - 3 H_\Lambda^{(3)}(N))) + 8 H_\Lambda(N)^5(144 H_0^2(-1 + \Omega_m + \Omega_r)H_\Lambda'(N) \\
&+ 146 H_\Lambda'(N)^3 + 18 H_\Lambda'(N)^2 H_\Lambda''(N) + H_0^2(-1 + \Omega_m + \Omega_r)(15 H_\Lambda''(N) - 6 H_\Lambda^{(3)}(N) - H_\Lambda^{(4)}(N))) \\
&+ 4 H_\Lambda(N)^4(540 H_0^2(-1 + \Omega_m + \Omega_r)H_\Lambda'(N)^2 + 124 H_\Lambda'(N)^4 + 12 H_\Lambda'(N)^3 H_\Lambda''(N) \\
&+ 3 H_0^2(-1 + \Omega_m + \Omega_r)H_\Lambda''(N)(17 H_\Lambda''(N) + 4 H_\Lambda^{(3)}(N)) + 2 H_0^2(-1 + \Omega_m + \Omega_r)H_\Lambda'(N)(129 H_\Lambda''(N) \\
&+ 12 H_\Lambda^{(3)}(N) - H_\Lambda^{(4)}(N))) - 2 H_\Lambda(N)^3(84 H_0^2(-1 + \Omega_m + \Omega_r)H_\Lambda'(N)^3 - 53 H_\Lambda'(N)^5 \\
&- 3 H_\Lambda'(N)^4 H_\Lambda''(N) + 21 H_0^2(-1 + \Omega_m + \Omega_r)H_\Lambda''(N)^3 + 3 H_0^2(-1 + \Omega_m + \Omega_r)H_\Lambda'(N)H_\Lambda''(N) \\
&\times (41 H_\Lambda''(N) - 4 H_\Lambda^{(3)}(N)) + H_0^2(-1 + \Omega_m + \Omega_r)H_\Lambda'(N)^2(217 H_\Lambda''(N) - 42 H_\Lambda^{(3)}(N) \\
&+ H_\Lambda^{(4)}(N)))))/(4 H_\Lambda(N)^4(2 H_\Lambda(N) + H_\Lambda'(N))^8),
\end{aligned}
\tag{A2}
$$

while for the Starobinsky model the first two terms are

$$
\frac{\delta H_2^2(N)}{H_0^2} = \frac{H_0^4(-1 + \Omega_{m0} + \Omega_{r0})^3(8 H_\Lambda(N)^2 + 9 H_\Lambda'(N)^2 + H_\Lambda(N)(34 H_\Lambda'(N) + 6 H_\Lambda''(N)))}{4 H_\Lambda(N)^2(2 H_\Lambda(N) + H_\Lambda'(N))^4},
\tag{A3}
$$

$$
\begin{aligned}
\frac{\delta H_4^2(N)}{H_0^2} = &-H_0^8(-1 + \Omega_{m0} + \Omega_{r0})^5(192 H_\Lambda(N)^8 - 486 H_0^2(-1 + \Omega_{m0} + \Omega_{r0})H_\Lambda'(N)^6 \\
&+ 320 H_\Lambda(N)^7(6 H_\Lambda'(N) - + H_\Lambda''(N)) - 18 H_0^2(-1 + \Omega_{m0} + \Omega_{r0})H_\Lambda(N)H_\Lambda'(N)^4(263 H_\Lambda'(N) + 48 H_\Lambda''(N)) \\
&+ 16 H_\Lambda(N)^6(32(-1 + \Omega_{m0} + \Omega_{r0}) + 5 H_\Lambda'(N)(47 H_\Lambda'(N) + 8 H_\Lambda''(N))) \\
&+ H_\Lambda(N)^2 H_\Lambda'(N)^2(-15562 H_0^2(-1 + \Omega_{m0} + \Omega_{r0})H_\Lambda'(N)^2 + 25 H_\Lambda'(N)^4 \\
&- 972 H_0^2(-1 + \Omega_{m0} + \Omega_{r0})H_\Lambda''(N)^2 - 12 H_0^2(-1 + \Omega_{m0} + \Omega_{r0})H_\Lambda'(N)(532 H_\Lambda''(N) - 15 H_\Lambda^{(3)}(N))) \\
&+ 4 H_\Lambda(N)^4(4422 H_0^2(-1 + \Omega_{m0} + \Omega_{r0})H_\Lambda'(N)^2 + 345 H_\Lambda'(N)^4 + 40 H_\Lambda'(N)^3 H_\Lambda''(N) \\
&+ 72 H_0^2(-1 + \Omega_{m0} + \Omega_{r0})H_\Lambda''(N)(9 H_\Lambda''(N) + 2 H_\Lambda^{(3)}(N)) + 18 H_0^2(-1 + \Omega_{m0} + \Omega_{r0})H_\Lambda'(N) \\
&\times (175 H_\Lambda''(N) + 20 H_\Lambda^{(3)}(N) - H_\Lambda^{(4)}(N))) + 2 H_\Lambda(N)^3(-7000 H_0^2(-1 + \Omega_{m0} + \Omega_{r0})H_\Lambda'(N)^3 \\
&+ 148 H_\Lambda'(N)^5 + 10 H_\Lambda'(N)^4 H_\Lambda''(N) - 324 H_0^2(-1 + \Omega_{m0} + \Omega_{r0})H_\Lambda''(N)^3 \\
&- 36 H_0^2(-1 + \Omega_{m0} + \Omega_{r0})H_\Lambda'(N)H_\Lambda''(N) \times (63 H_\Lambda''(N) - 4 H_\Lambda^{(3)}(N)) \\
&- 9 H_0^2(-1 + \Omega_{m0} + \Omega_{r0})H_\Lambda'(N)^2(609 H_\Lambda''(N) - 66 H_\Lambda^{(3)}(N) + H_\Lambda^{(4)}(N))) \\
&+ 8 H_\Lambda(N)^5(824 H_0^2(-1 + \Omega_{m0} + \Omega_{r0})H_\Lambda'(N) + 400 H_\Lambda'(N)^3 + 60 H_\Lambda'(N)^2 H_\Lambda''(N) \\
&+ 3 H_0^2(-1 + \Omega_{m0} + \Omega_{r0}) \times (29 H_\Lambda''(N) - 3(6 H_\Lambda^{(3)}(N) + H_\Lambda^{(4)}(N)))))/(16 H_\Lambda(N)^6(2 H_\Lambda(N) + H_\Lambda'(N))^{10}).
\end{aligned}
\tag{A4}
$$

[1] M. Tegmark *et al.*, Astrophys. J. **606**, 702 (2004).
[2] D. N. Spergel *et al.*, Astrophys. J. Suppl. Ser. **170**, 377 (2007).
[3] T. M. Davis *et al.*, Astrophys. J. **666**, 716 (2007).
[4] M. Kowalski *et al.*, Astrophys. J. **686**, 749 (2008).
[5] M. Hicken *et al.*, Astrophys. J. **700**, 1097 (2009).
[6] E. Komatsu *et al.*, Astrophys. J. Suppl. Ser. **180**, 330 (2009); G. Hinshaw *et al.*, Astrophys. J. Suppl. Ser. **180**, 225 (2009).

 [7] J. A. S. Lima and J. S. Alcaniz, Mon. Not. R. Astron. Soc. **317**, 893 (2000); J. F. Jesus and J. V. Cunha, Astrophys. J. Lett. **690**, L85 (2009).

 [8] S. Basilakos and M. Plionis, Astrophys. J. Lett. **714**, L185 (2010).

 [9] E. Komatsu *et al.*, Astrophys. J. Suppl. Ser. **192**, 18 (2011).

[10] T. P. Sotiriou and V. Faraoni, Rev. Mod. Phys. **82**, 451 (2010).

[11] A. A. Starobinsky, Phys. Lett. **91B**, 99 (1980).

[12] S. M. Carrol, V. Duvvuri, M. Trodden, and M. S. Turner, Phys. Rev. D **70**, 043528 (2004).

[13] A. D. Dolgov and M. Kawasaki, Phys. Lett. B **573**, 1 (2003); T. Chiba, Phys. Lett. B **575**, 1 (2003); G. Allemandi, A. Borowiec, M. Francaviglia, and S. D. Odintsov, Phys. Rev. D **72**, 063505 (2005); A. L. Erickcek, T. L. Smith, and M. Kamionkowski, Phys. Rev. D **74**, 121501 (2006); T. Chiba, T. L. Smith, and A. L. Erickcek, Phys. Rev. D **75**, 124014 (2007); W. Hu and I. Sawicki, Phys. Rev. D **76**, 064004 (2007); S. A. Appleby and R. A. Battye, Phys. Lett. B **654**, 7 (2007); J. Santos, J. S. Alcaniz, F. C. Carvalho, and N. Pires, Phys. Lett. B **669**, 14 (2008); J. Santos and M. J. Reboucas, Phys. Rev. D **80**, 063009 (2009); V. Miranda, S. E. Joras, I. Waga, and M. Quartin, Phys. Rev. Lett. **102**, 221101 (2009); S. H. Pereira, C. H. G. Bessa, and J. A. S. Lima, Phys. Lett. B **690**, 103 (2010); R. Reyes, R. Mandelbaum, U. Seljak, T. Baldauf, J. E. Gunn, L. Lombriser, and R. E. Smith, Nature (London) **464**, 256 (2010); S. Capozziello, V. F. Cardone, and V. Salzano, Phys. Rev. D **78**, 063504 (2008); A. Aviles, A. Bravetti, S. Capozziello, and O. Luongo, Phys. Rev. D **87**, 044012 (2013); S. Capozziello and M. De Laurentis, Phys. Rep. **509**, 167 (2011).

[14] L. Amendola, D. Polarski, and S. Tsujikawa, Phys. Rev. Lett. **98**, 131302 (2007); L. Amendola, R. Gannouji, D. Polarski, and S. Tsujikawa, Phys. Rev. D **75**, 083504 (2007).

[15] E. J. Copeland, M. Sami, and S. Tsujikawa, Int. J. Mod. Phys. D **15**, 1753 (2006); L. Amendola and S. Tsujikawa, *Dark Energy Theory and Observations* (Cambridge University Press, Cambridge, 2010); R. R. Caldwell and M. Kamionkowski, Annu. Rev. Nucl. Part. Sci. **59**, 397 (2009); I. Sawicki and W. Hu, Phys. Rev. D **75**, 127502 (2007).

[16] G. Dvali, G. Gabadadze, and M. Porrati, Phys. Lett. B **485**, 208 (2000).

[17] P. C. Stavrinos, A. Kouretsis, and M. Stathakopoulos, Gen. Relativ. Gravit. **40**, 1403 (2008); J. Skalala and M. Visser, Int. J. Mod. Phys. D **19**, 1119 (2010); N. Mavromatos, S. Sarkar, and A. Vergou, Phys. Lett. B **696**, 300 (2011); S. Vacaru, Int. J. Mod. Phys. D **21**, 1250072 (2012); M. C. Werener, Gen. Relativ. Gravit. **44**, 3047 (2012).

[18] J. P. Uzan, Phys. Rev. D **59**, 123510 (1999); L. Amendola, Phys. Rev. D **60**, 043501 (1999); T. Chiba, Phys. Rev. D **60**, 083508 (1999); N. Bartolo and M. Pietroni, Phys. Rev. D **61**, 023518 (1999); F. Perrotta, C. Baccigalupi, and S. Matarrese, Phys. Rev. D **61**, 023507 (1999); B. Boisseau, G. Esposito-Farese, D. Polarski, and A. A. Starobinsky, Phys. Rev. Lett. **85**, 2236 (2000); G. Esposito-Farese and D. Polarski, Phys. Rev. D **63**, 063504 (2001); D. F. Torres,

Phys. Rev. D **66**, 04522 (2002); Y. Fujii and K. Maeda, *The Scalar-Tensor Theory of Gravitation* (Cambridge University Press, Cambridge, 2003).

[19] S. Nojiri, S. D. Odintsov, and M. Sasaki, Phys. Rev. D **72**, 023003 (2005); D. Comelli, Phys. Rev. D **72**, 064018 (2005); I. Neupane and B. M. N. Carter, J. Cosmol. Astropart. Phys. 06 (2006) 004; T. Koivisto and D. F. Mota, Phys. Lett. B **644**, 104 (2007); F. Bauer, J. Solà, and H. Štefančić, J. Cosmol. Astropart. Phys. 12 (2010) 029; F. Bauer, J. Solà, and H. Štefančić, Phys. Lett. B **688**, 269 (2010).

[20] W. Hu and I. Sawicki, Phys. Rev. D **76**, 064004 (2007).

[21] A. A. Starobinsky, JETP Lett. **86**, 157 (2007).

[22] K. Bamba, A. Lopez-Revelles, R. Myrzakulov, S. D. Odintsov, and L. Sebastiani, Classical Quantum Gravity **30**, 015008 (2013).

[23] E. V. Linder, Phys. Rev. D **70**, 023511 (2004); E. V. Linder and R. N. Cahn, Astropart. Phys. **28**, 481 (2007).

[24] V. Silveira and I. Waga, Phys. Rev. D **50**, 4890 (1994).

[25] L. Wang and J. P. Steinhardt, Astrophys. J. **508**, 483 (1998).

[26] S. Nesseris and L. Perivolaropoulos, Phys. Rev. D **77**, 023504 (2008).

[27] Y. Gong, Phys. Rev. D **78**, 123010 (2008).

[28] H. Wei, Phys. Lett. B **664**, 1 (2008).

[29] Y. G. Gong, Phys. Rev. D **78**, 123010 (2008); X. Fu, P. Wu, and H. Yu, Phys. Lett. B **677**, 12 (2009).

[30] R. Gannouji, B. Moraes, and D. Polarski, J. Cosmol. Astropart. Phys. 02 (2009) 034.

[31] S. Tsujikawa, R. Gannouji, B. Moraes, and D. Polarski, Phys. Rev. D **80**, 084044 (2009).

[32] S. Basilakos and P. Stavrinos, Phys. Rev. D **87**, 043506 (2013).

[33] L. Guzzo *et al.*, Nature (London) **451**, 541 (2008).

[34] C. Di Porto and L. Amendola, Phys. Rev. D **77**, 083508 (2008).

[35] J. Dosset, M. Ishak, J. Moldenhauer, Y. Gong, and A. Wang, J. Cosmol. Astropart. Phys. 04 (2010) 022.

[36] S. Basilakos and A. Pouri, Mon. Not. R. Astron. Soc. **423**, 3761 (2012).

[37] M. J. Hudson and S. J. Turnbull, Astrophys. J. Lett. **751**, L30 (2012).

[38] S. Basilakos, Int. J. Mod. Phys. D **21**, 1250064 (2012).

[39] L. Samushia *et al.*, Mon. Not. R. Astron. Soc. **429**, 1514 (2013).

[40] A. Vikhlinin *et al.*, Astrophys. J. **692**, 1060 (2009).

[41] D. Rapetti, S. W. Allen, A. Mantz, and H. Ebeling, Mon. Not. R. Astron. Soc. **406**, 179 (2010).

[42] S. A. Thomas, F. B. Abdalla, and J. Weller, Mon. Not. R. Astron. Soc. **395**, 197 (2009); S. F. Daniel, E. V. Linder, T. L. Smith, R. R. Caldwell, A. Cooray, A. Leauthaud, and L. Lombriser, Phys. Rev. D **81**, 123508 (2010); R. Bean and M. Tangmatitham, Phys. Rev. D **81**, 083534 (2010).

[43] E. Gaztanaga, M. Eriksen, M. Crocce, F. J. Castander, P. Fosalba, P. Marti, R. Miquel, and A. Cabré, Mon. Not. R. Astron. Soc. **422**, 2904 (2012).

[44] S. Nesseris and J. Garcia-Bellido, J. Cosmol. Astropart. Phys. 11 (2012) 033.

[45] F. Beutler, C. Blake, M. Colless, D. H. Jones, L. Staveley-Smith, G. B. Poole, L. Campbell, Q. Parker, W. Saunders, and F. Watson, Mon. Not. R. Astron. Soc. **423**, 3430 (2012).

[46] D. Polarski and R. Gannouji, Phys. Lett. B **660**, 439 (2008).

[47] N. Suzuki *et al.*, Astrophys. J. **746**, 85 (2012).

[48] W. J. Percival, Mon. Not. R. Astron. Soc. **401**, 2148 (2010).

[49] T. D. Saini, S. Raychaudhury, V. Sahni, and A. A. Starobinsky, Phys. Rev. Lett. **85**, 1162 (2000); D. Huterer and M. S. Turner, Phys. Rev. D **64**, 123527 (2001).

[50] S. Capozziello and S. Tsujikawa, Phys. Rev. D **77**, 107501 (2008).

[51] X. Fu, P. Wu, and H. Yu, Eur. Phys. J. C **68**, 271 (2010).

[52] A. A. Starobinsky, JETP Lett. **86**, 157 (2007).

[53] R. Dave, R. R. Caldwell, and P. J. Steinhardt, Phys. Rev. D **66**, 023516 (2002)

[54] A. Lue, R. Scossimarro, and G. D. Starkman, Phys. Rev. D **69**, 124015 (2004).

[55] E. V. Linder, Phys. Rev. D **72**, 043529 (2005).

[56] F. H. Stabenau and B. Jain, Phys. Rev. D **74**, 084007 (2006).

[57] P. J. Uzan, Gen. Relativ. Gravit. **39**, 307 (2007).

[58] S. Tsujikawa, K. Uddin, and R. Tavakol, Phys. Rev. D **77**, 043007 (2008).

[59] J. B. Dent, S. Dutta, and L. Perivolaropoulos, Phys. Rev. D **80**, 023514 (2009).

[60] P. J. E. Peebles, *Principles of Physical Cosmology* (Princeton University Press, Princeton, New Jersey, 1993).

[61] W.-S. Zhang, C. Cheng, Q. Huang, M. Li, S. Li, X. Li, and S. Wang, Sci. China Phys. Mech. Astron. **55**, 2244 (2012).

[62] A. B. Belloso, J. Garcia-Bellido, and D. Sapone, J. Cosmol. Astropart. Phys. 10 (2011) 010.

[63] C. Di Porto, L. Amendola, and E. Branchini, Mon. Not. R. Astron. Soc. **419**, 985 (2012).

[64] M. Ishak and J. Dosset, Phys. Rev. D **80**, 043004 (2009).

[65] R. E. Smith, J. A. Peacock, A. Jenkins, S. D. M. White, C. S. Frenk, F. R. Pearce, P. A. Thomas, G. Efstathiou, and

H. M. P. Couchman, (Virgo Consortium Collaboration), Mon. Not. R. Astron. Soc. **341**, 1311 (2003).

[66] M. Tegmark *et al.* (SDSS Collaboration), Astrophys. J. **606**, 702 (2004).

[67] W. J. Percival *et al.*, Astrophys. J. **657**, 645 (2007).

[68] R. Angulo, C. M. Baugh, C. S. Frenk, and C. G. Lacey, Mon. Not. R. Astron. Soc. **383**, 755 (2008).

[69] Y-S. Song and W. J. Percival, J. Cosmol. Astropart. Phys. 10 (2009) 004.

[70] W. J. Percival *et al.*, Mon. Not. R. Astron. Soc. **353**, 1201 (2004).

[71] M. Tegmark *et al.*, Phys. Rev. D **74**, 123507 (2006).

[72] L. Samushia, W. J. Percival, and A. Raccanelli, Mon. Not. R. Astron. Soc. **420**, 2102 (2012).

[73] C. Blake *et al.*, Mon. Not. R. Astron. Soc. **415**, 2876 (2011).

[74] B. A. Reid *et al.*, Mon. Not. R. Astron. Soc. **426**, 2719 (2012).

[75] R. Tojeiro, *et al.*, Mon. Not. R. Astron. Soc. **424**, 2339 (2012).

[76] http://supernova.lbl.gov/Union/.

[77] C. Blake *et al.*, Mon. Not. R. Astron. Soc. **418**, 1707 (2011).

[78] G. Hinshaw *et al.*, arXiv:1212.5226.

[79] W. Hu and N. Sugiyama, Astrophys. J. **471**, 542 (1996).

[80] A. Melchiorri, L. Mersini, C. Ödman, and M. Trodden, Phys. Rev. D **68**, 043509 (2003); S. Nesseris and L. Perivolaropoulos, J. Cosmol. Astropart. Phys. 01 (2007) 018.

[81] H. Akaike, IEEE Trans. Automatic Control **19**, 716 (1974); N. Sugiura, Commun. Stat. A **7**, 13 (1978).

[82] O. Elgaroy and T. Multamaki, J. Cosmol. Astropart. Phys. 09 (2009) 2; P. S. Corasaniti and A. Melchiorri, Phys. Rev. D **77**, 103507 (2008).

[83] Y. Akrami, C. Savage, P. Scott, J. Conrad, and J. Edsjo, J. Cosmol. Astropart. Phys. 07 (2011) 002.

[84] http://leandros.physics.uoi.gr/fr-constraints/probes.htm.